

# Dark matter, density perturbations and structure formation

A. Del Popolo<sup>1,2,3</sup>

<sup>1</sup>*Boğaziçi University, Physics Department, 80815 Bebek, Istanbul, Turkey*

<sup>2</sup>*Dipartimento di Matematica, Università Statale di Bergamo, via dei Caniana, 2, 24127, Bergamo, ITALY*

<sup>3</sup>*Istanbul Technical University, Ayazaga Campus, Faculty of Science and Letters, 34469 Maslak/ISTANBUL, Turkey*

**Abstract**—This paper provides a review of the variants of dark matter which are thought to be fundamental components of the universe and their role in origin and evolution of structures and some new original results concerning improvements to the spherical collapse model. In particular, I show how the spherical collapse model is modified when we take into account dynamical friction and tidal torques.

## 1. INTRODUCTION

The origin and evolution of large scale structure is today the outstanding problem in cosmology. This is the most fundamental question we can ask about the universe whose solution should help us to better understand problems as the epoch of galaxy formation, the clustering in the galaxy distribution, the amplitude and form of anisotropies in the microwave background radiation. Several has been the approaches and models trying to attack and solve this problem: no one has given a final answer.

The leading idea of all structure formation theories is that structures was born from small perturbations in the otherwise uniform distribution of matter in the early Universe, which is supposed to be, in great part, dark (matter not detectable through light emission).

With the term Dark Matter cosmologists indicate an hypothetic material component of the universe which does not emit directly electromagnetic radiation (unless it decays in particles having this property ([1], but also see [2])).

Dark matter, cannot be revealed directly, but nevertheless it is necessary to postulate its existence in order to explain the discrepancies between the observed dynamical properties of galaxies and clusters of galaxies and the theoretical predictions based upon models of these objects assuming that the only matter present is the visible one. If in the space were present a diffused material component having gravitational mass, but unable to emit electromagnetic radiation in significative quantity, this discrepancy could be eliminated ([3]). The study of Dark Matter has as its finality the explanation of formation of galaxies and in general of cosmic structures. For this reason, in the last decades, the origin of cosmic structures has been “framed” in models in which Dark Matter constitutes the skeleton of cosmic structures and supply the most part of the mass of which the same is made.

There are essentially two ways in which matter in the universe can be revealed: by means of radiation, by itself emitted, or by means of its gravitational interaction with baryonic matter which gives rise to cosmic structures. Electromagnetic radiation permits to reveal only baryonic matter. In the second case, we can only tell that we are in presence of matter that interacts by means of gravitation with the luminous mass in the universe. The original hypotheses on Dark Matter go back to measures performed by Oort ([4]) of the surface density of matter in the galactic disk, which was obtained through the study of the stars motion in direction orthogonal to the galactic plane. The result obtained by Oort, which was after him named “Oort Limit”, gave a value of  $\rho = 0.15 M_{\odot} pc^{-3}$  for the mass density, and a mass, in the region studied, superior to that present in stars. Nowadays, we know that the quoted discrepancy is due to the presence of HI in the solar

clusters (e.g. Coma Cluster) and the total mass contained in galaxies of the same clusters. These and other researches from the thirties to now, have confirmed that a great part of the mass in the universe does not emit radiation that can be directly observed.

### 1.1 Determination of $\Omega$ and Dark Matter

The simplest cosmological model that describes, in a sufficient coherent manner, the evolution of the universe, from  $10^{-2}s$  after the initial singularity to now, is the so called *Standard Cosmological Model* (or Hot Big Bang model). It is based upon the Friedmann-Robertson-Walker (FRW) metric, which is given by:

$$ds^2 = c^2 dt^2 - a(t)^2 \left[ \frac{dr^2}{1 - kr^2} + r^2(d\theta^2 + \sin\theta^2 d\phi^2) \right] \quad (1)$$

where  $c$  is the light velocity,  $a(t)$  a function of time, or a scale factor called “expansion parameter”,  $t$  is the time co-ordinate,  $r$ ,  $\theta$  and  $\phi$  the comoving space coordinates. The evolution of the universe is described by the parameter  $a(t)$  and it is fundamentally connected to the value  $\rho$  of the average density.

The equations that describe the dynamics of the universe are the Friedmann’s equations ([7]) that we are going to introduce in a while. These equations can be obtained starting from the equations of the gravitational field of Einstein ([8]):

$$R_{ik} - \frac{1}{2}g_{ik}R = -\frac{8\pi G}{c^4}T_{ik} \quad (2)$$

where now,  $R_{ik}$  is a symmetric tensor, also known as Ricci tensor, which describes the geometric properties of space-time,  $g_{ik}$  is the metric tensor,  $R$  is the scalar curvature,  $T_{ik}$  is the energy-momentum tensor.

These equations connect the properties of space-time to the mass-energy. In other terms they describe how space-time is modeled by mass. Combining Einstein equations to the FRW metric leads to the dynamic equations for the expansion parameter,  $a(t)$ . These last are the Friedmann equations:

$$d(\rho a^3) = -pd(a^3) \quad (3)$$

$$\frac{1}{a^2}\dot{a}^2 + \frac{k}{a^2} = \frac{8\pi G}{3}\rho \quad (4)$$

$$2\frac{\ddot{a}}{a} + \frac{\dot{a}^2}{a^2} + \frac{k}{a^2} = -8\pi G\rho \quad (5)$$

where  $p$  is the pressure of the fluid of which the universe is constituted,  $k$  is the curvature parameter and  $a(t)$

the components of the today universe are galaxies. If we assume that galaxies motion satisfy Weyl ([9]) postulate, the velocity vector of a galaxy is given by  $u^i = (1, 0, 0, 0)$ , and then the system behaves as a system made of dust for which we have  $p = 0$ . Only two of the three Friedmann equations are independent, because the first connects density,  $\rho$  to the expansion parameter  $a(t)$ . The character of the solutions of these equations depends on the value of the curvature parameter,  $k$ , which is also determined by the initial conditions by means of Eq. 3. The solution to the equations now written shows that if  $\rho$  is larger than  $\rho_c = \frac{3H^2}{8\pi G} = 1.88 * 10^{-29} g/cm^3$  (critical density, which can be obtained from Friedmann equations putting  $t = t_0$ ,  $k = 0$ , and  $H = 100 km/sMpc$ ), space-time has a closed structure ( $k = 1$ ) and equations shows that the system go through a singularity in a finite time. This means that the universe has an expansion phase until it reaches a maximum expansion after which it recollapse. If  $\rho < \rho_c$ , the expansion never stops and the universe is open  $k = -1$  (the universe has a structure similar to that of an hyperboloid, in the two-dimensional case). If finally,  $\rho = \rho_c$  the expansion is decelerated and has infinite duration in time,  $k = 0$ , and the universe is flat (as a plane in the two-dimensional case). The concept discussed can be expressed using the parameter  $\Omega = \frac{\rho}{\rho_c}$ . In this case, the condition  $\Omega = 1$  corresponds to  $k = 0$ ,  $\Omega < 1$  corresponds to  $k = -1$ , and  $\Omega > 1$  corresponds to  $k = 1$ .<sup>1</sup>

The value of  $\Omega$  can be calculated in several ways. The most common methods are the dynamical methods, in which the effects of gravity are used, and kinematics methods sensible to the evolution of the scale factor and to the space-time geometry. The results obtained for  $\Omega$  with these different methods are summarized in the following.

#### *Dynamical methods:*

(a) *Rotation curves:* The contribution of spiral galaxies to the density in the universe is calculated by using their rotation curves and the third Kepler law. Using the last it is possible to obtain the mass of a spiral galaxy from the equation:

$$M(r) = v^2 r / G \quad (6)$$

where  $v$  is the velocity of a test particle at a distance  $r$  from the center and  $M(r)$  is the mass internal to the circular orbit of the particle. In order to determine the mass  $M$  is necessary to have knowledge of the term  $v^2$  in Eq. (6) and this can be done from the study of the rotation curves through the 21 cm line of HI. Rotation curves of galaxies are characterized by a peak reached at distances of some Kpcs and a behavior typically flat for the regions at distance larger than that of the peak. A peculiarity is that the expected Keplerian fall is not observed. This result is consistent with extended haloes containing masses till 10 times the galactic mass observed in the optical ([10]). The previous result is obtained assuming that the halo mass obtained with this method is distributed in a spherical region so that we can use Eq. (6) and that we neglect the tidal interaction with the neighboring galaxies which tend to produce an expansion of the halo. After  $M$  and the luminosity of a series of elliptical galaxies is determined, the contribution to the density of the universe

is given by  $\rho = \langle \frac{M}{L} \rangle > \ell$  where  $\ell$  is the luminosity per unit volume due to galaxies and can be obtained from the galactic luminosity function  $\phi(L)dL$ , which describes the number of galaxies per  $Mpc^3$  and luminosity range  $L, L + dL$ . The value that is usually assumed for  $\ell$  is  $\ell = 2.4h10^8 L_{bo} Mpc^{-3}$ . The arguments used lead to a value of  $\Omega_g$  for the luminous parts of spiral galaxies of  $\Omega_g \leq 0.01$ , while for haloes  $\Omega_h \geq 0.03 - 0.1$ . The result shows that the halo mass is noteworthy larger than the galactic mass observable in the optical ([11]).

#### (b) *Virial theorem:*

In the case of non spiral galaxies and clusters, the mass can be obtained using the virial theorem  $2T + V = 0$ , with

$$T \cong \frac{3}{2} M \langle v_r^2 \rangle \quad (7)$$

where  $\langle v_r^2 \rangle$  is the velocity dispersion along the line of sight. After getting the value of  $M$  of the cluster by means of the virial theorem one determines  $L$  by means of observations. Given  $M$  and  $L$ , the value of  $\Omega$  for clusters is obtained similarly to the case of spiral galaxies. Usual values obtained for  $\Omega$  are  $\Omega = 0.1 - 0.3$  ([11]). A problem of the quoted method is that in general the results obtained are the right one only for virialized, spherically symmetric clusters. In general, clusters are not virialized objects: even Coma clusters seems to have a central core constituted by more than one blob of mass ([12]).

#### (c) *Peculiar velocities:*

The velocity of a galaxy can be written as:

$$\mathbf{V}_g = H\mathbf{r} + \delta\mathbf{v} \quad (8)$$

where  $H$  is Hubble constant. The previous equation shows that the motion of a galaxy is constituted by two components: the velocity of the galaxy due to the Hubble flow and a peculiar velocity  $\delta\mathbf{v}$ , which describes the motion of the galaxy with respect to the background. In the linear regime, as we see in a while, we find that on average on a scale of length  $\lambda$ , it is:

$$\frac{\delta v}{c} \approx \Omega^{0.6} \frac{\lambda}{H_0^{-1}} \frac{\delta \rho}{\rho} \quad (9)$$

([13]). Then given the overdensity  $\frac{\delta \rho}{\rho}$  on scale  $\lambda$  and  $\delta v$ , it is possible to obtain  $\Omega$ . The overdensity  $\frac{\delta \rho}{\rho}$  can be obtained from the overdensity of galaxies  $\frac{\delta n_g}{n_g}$  using the relation  $\frac{\delta \rho}{\rho} = \frac{\delta n_g}{n_g} b^{-1}$  with  $1 < b < 3$ . Using IRAS catalog in order to obtain the overdensity in galaxies one finds  $\Omega \cong 1$ . The values of  $\Omega$  obtained using the method of peculiar velocity assume that the peculiar velocity fields describe in an accurate way, the inhomogeneity in the distribution of underlying mass. We should note that the peculiar velocity method has some difficulties. In general, in order to obtain these last it is necessary to determine the redshift and the distance of galaxies and by using these data it is possible to obtain the peculiar velocity:

$$v_{pec} = zc - H_0 d \quad (10)$$

It is evident that there are problems in measuring the distance  $d$ , problems connected to difficulties in finding trustworthy indicators of distance. Moreover the peculiar

(d) *Kinematic methods:*

These methods are based upon the use of relations between physical quantities dependent on cosmological parameters. An example of those relations is the relation luminosity distance-redshift:

$$H_0 d_L = z + \frac{1}{2}(1 - q_0)z^2 \quad (11)$$

where  $H_0$  is Hubble constant nowadays,  $z$  is the redshift,  $d_L = \frac{4\pi L}{F}$  the luminosity distance,  $L$  the absolute luminosity, and  $F$  the flux. By means of the relations luminosity-redshift, angle-redshift, number of objects-redshift, it is possible to determine the parameter of deceleration  $q_0 = -\frac{\ddot{a}_0}{H_0^2 a_0}$  ( $a_0$  and  $H_0 = \frac{\dot{a}_0}{a_0} = 100 h km/Mpc$  are the scale factor and the Hubble constant, nowadays). At the same time  $q_0$  is connected to  $\Omega$  by means of  $q_0 = \frac{\Omega}{2}$ , in a matter universe. One of the first test used, the luminosity distance-redshift has several problems due to effects of the evolution of sources. Uncertainties in the knowledge of the effects of galactic evolution on the intrinsic luminosity of the same has not, in the past, permitted to find definitive values of  $q_0$ . For this reason, [14] introduced another kinematic test: number of galaxies-redshift. This test is based on the count of the number of galaxies in a comoving element of galaxies, defined by the surface  $d\Omega$  and the redshift  $dz$ . This number depends on  $q_0$ . Nevertheless the effects of evolution of sources influences on the results of the test, it is more sensible to the evolution of number of sources than to the evolution of luminosity, on which there is not an accepted theory. Results gives high values of  $\Omega$  ( $\Omega = 0.9^{+0.7}_{-0.5}$ ) ([13]).<sup>2</sup>

(e) *Primordial nucleosynthesis:*

The theory of primordial nucleosynthesis, proposed in 1946 by Gamov, assumes that the light elements till  $Li_7$  are generated after big bang and that heavier elements originate from nuclear reactions inside stars. The values obtained for the abundances depends on some parameters like:  $\eta$ , the value of the ratio baryons-photons, nowadays;  $N_\nu$ , the number of neutrinos species;  $T_{CMBR}$ , the temperature of Cosmic Microwave Background Radiation. The theory of primordial nucleosynthesis permits to give limits to  $\Omega_b$  ( $b$  stands for baryons). With a ratio baryons-photons  $3 * 10^{-10} \leq \eta \leq 5 * 10^{-10}$ , and a value of  $N_\nu \leq 4$  for the neutrinos species,  $T_{CMBR} = 2.736 \pm 0.01 K$ , is found  $0.011 \leq \Omega_b \leq 0.12$  ([13]).

In the following, we summarize the results of some more recent results.

[16] used several methods to obtain the value of  $\Omega$ . According to their classification, we divide the methods into the following four classes:

- *Global measures.* Based on properties of space-time that constrain combinations of  $\Omega_m$  and the other cosmological parameters ( $\Lambda$ ,  $H_0$ ,  $t_0$ ).
- *Virialized Systems.* Methods based on nonlinear dynamics within galaxies and clusters on comoving scales  $1 - 10 h^{-1} Mpc$ .
- *Large-scale structure.* Measurements based on mildly-nonlinear gravitational dynamics of fluctuations on scales  $10 - 100 h^{-1} Mpc$  of superclusters and voids, in particular *cosmic flows*.

- *Growth rate of fluctuations.* Comparisons of present day structure with fluctuations at the last scattering of the cosmic microwave background (CMB) or with high redshift objects of the young universe.

The methods and current estimates are summarized in Table 3. The estimates based on virialized objects typically yield low values of  $\Omega_m \sim 0.2 - 0.3$ . The global measures, large-scale structure and cosmic flows typically indicate higher values of  $\Omega_m \sim 0.4 - 1$ .

Bahcall et al. ([17]), showed that the evolution of the number density of rich clusters of galaxies breaks the degeneracy between  $\Omega$  (the mass density ratio of the universe) and  $\sigma_8$  (the normalization of the power spectrum),  $\sigma_8 \Omega^{0.5} \simeq 0.5$ , that follows from the observed present-day abundance of rich clusters. The evolution of high-mass (Coma-like) clusters is strong in  $\Omega = 1$ , low- $\sigma_8$  models (such as the standard biased CDM model with  $\sigma_8 \simeq 0.5$ ), where the number density of clusters decreases by a factor of  $\sim 10^3$  from  $z = 0$  to  $z \simeq 0.5$ ; the same clusters show only mild evolution in low- $\Omega$ , high- $\sigma_8$  models, where the decrease is a factor of  $\sim 10$ . This diagnostic provides a most powerful constraint on  $\Omega$ . Using observations of clusters to  $z \simeq 0.5 - 1$ , the authors found only mild evolution in the observed cluster abundance, and  $\Omega = 0.3 \pm 0.1$  and  $\sigma_8 = 0.85 \pm 0.15$  (for  $\Lambda = 0$  models; for  $\Omega + \Lambda = 1$  models,  $\Omega = 0.34 \pm 0.13$ ).

ferreira et al. ([18]), proposed an alternative method to estimate  $v_{12}$  directly from peculiar velocity samples, which contain redshift-independent distances as well as galaxy redshifts. In contrast to other dynamical measures which determine  $\beta \equiv \Omega^{0.6} \sigma_8$ , this method can provide an estimate of  $\Omega^{0.6} \sigma_8^2$  for a range of  $\sigma_8$  where  $\Omega$  is the cosmological density parameter, while  $\sigma_8$  is the standard normalization for the power spectrum of density fluctuations.

Melchiorri ([19]), used the angular power spectrum of the Cosmic Microwave Background, measured during the North American test flight of the BOOMERANG experiment, to constrain the geometry of the universe. Within the class of Cold Dark Matter models, they find that the overall fractional energy density of the universe,  $\Omega$ , is constrained to be  $0.85 \leq \Omega \leq 1.25$  at the 68% confidence level.

Branchini ([20]), compared the density and velocity fields as extracted from the Abell/ACO clusters to the corresponding fields recovered by the POTENT method from the Mark III peculiar velocities of galaxies. Quantitative comparisons within a volume containing  $\sim 12$  independent samples yield  $\beta_c \equiv \Omega^{0.6}/b_c = 0.22 \pm 0.08$ , where  $b_c$  is the cluster biasing parameter at  $15 h^{-1} Mpc$ . If  $b_c \sim 4.5$ , as indicated by the cluster correlation function, their result is consistent with  $\Omega \sim 1$ .

(f) *Inflation:*

It is widely supposed that the very early universe experienced an era of inflation (see [21], [22], [13]). By ‘inflation’ one means that the scale factor has positive acceleration,  $\ddot{a} > 0$ , corresponding to repulsive gravity and  $3p < -\rho$ . During inflation  $aH = \dot{a}$  is increasing, so that comoving scales are leaving the horizon (Hubble distance) rather than entering it, and it is supposed that at the beginning of inflation the observable universe was well within the horizon.

The inflationary hypothesis is attractive because it holds out the possibility of calculating cosmological quantities, given the Lagrangian describing the fundamental interactions. The Standard Model, describing the interactions up to energies of order  $1 TeV$ , is not viable in this context because it does not permit inflation, but this should not be regarded as a serious setback because it is universally agreed that the Standard Model will be replaced by a more complete theory.

mology. The nature of the required extension is not yet known, though it is conceivable that it could become known in the foreseeable future. But even without a specific model of the interactions (ie., a specific Lagrangian), the inflationary hypothesis can still offer guidance about what to expect in cosmology. More dramatically, one can turn around the theory-to-observation sequence, to rule out otherwise reasonable models. The importance of inflation is connected to:

a) the origin of density perturbations, which could originate during inflation as quantum fluctuations, which become classical as they leave the horizon and remain so on re-entry. The original quantum fluctuations are of exactly the same type as those of the electromagnetic field, which give rise to the experimentally observed Casimir effect.

b) One of the most dramatic and simple effects is that there is no fine-tuning of the initial value of the density parameter  $\Omega = 8\pi\rho/3m_{Pl}^2H^2$ . From the Friedmann equation,  $\Omega$  is given by

$$\Omega - 1 = \left(\frac{K}{aH}\right)^2 \quad (12)$$

Its present value  $\Omega_0$  is certainly within an order of magnitude of 1, and in the absence of an inflationary era  $\Omega$  becomes ever smaller as one goes back in time, implying an initial fine tuning. In contrast, if there is an inflationary era beginning when the observable universe is within the horizon, Eq. (12) implies that  $\Omega_0$  will be of order 1, provided only that the same is true of  $\Omega$  at the beginning of inflation. A value of  $\Omega_0$  extremely close to 1 is the most natural, though it is not mandatory.<sup>3</sup>

c) Another effect of inflation is that it can eliminate particles and topological defects which would otherwise be present. Anything produced before inflation is diluted away, and after inflation there is a maximum temperature (the ‘reheat’ temperature) which is not high enough to produce all the particles and defects that might otherwise be present. As we shall remark later, this mechanism can remove desirable, as well as undesirable, objects.

d) The most dramatic effect of inflation is that it may offer a way of understanding the homogeneity and isotropy of the universe, or at any rate of significant regions of it. We have nothing to say about this complex issue in its full generality, but a more modest version of it is our central concern. In this version, one begins the discussion at some early stage of inflation, when the universe is supposed already to be *approximately* homogeneous and isotropic. One then argues that in that case, scales far inside the horizon must be *absolutely* homogeneous and isotropic, except for the effect of vacuum fluctuations in the fields. Finally, one shows that after they leave the horizon, such fluctuations can become the classical perturbations that one deals with in cosmological perturbation theory. This possibility was first pointed out for gravitational waves by [23] and for density perturbations by several people ([24]; [25]; [26]). As we shall go to some trouble to demonstrate, the vacuum fluctuations can be evaluated unambiguously once an inflationary model is specified.

(g) *Scalar field inflation:*

Two mechanisms for inflation have been proposed. The

simplest one ([21]) invokes a scalar field, termed the inflaton field. An alternative ([23]) is to invoke a modification of Einstein gravity, and combinations of the two mechanisms have also been proposed. During inflation however, the proposed modifications of gravity can be abolished by redefining the spacetime metric tensor, so that one recovers the scalar field case. We focus on it for the moment, but modified gravity models will be included later in our survey of specific models.

In comoving coordinates a homogeneous scalar field  $\phi$  with minimal coupling to gravity has the equation of motion

$$\ddot{\phi} + 3H\dot{\phi} + V'(\phi) = 0 \quad (13)$$

Its energy density and pressure are

$$\rho = V + \frac{1}{2}\dot{\phi}^2 \quad (14)$$

$$p = -V + \frac{1}{2}\dot{\phi}^2 \quad (15)$$

If such a field dominates  $\rho$  and  $p$ , the inflationary condition  $3p < \rho$  is achieved provided that the field rolls sufficiently slowly,

$$\dot{\phi}^2 < V \quad (16)$$

Practically all of the usually considered models of inflation satisfy three conditions. First, the motion of the field is overdamped, so that the ‘force’  $V'$  balances the ‘friction term’  $3H\dot{\phi}$ ,

$$\dot{\phi} \simeq -\frac{1}{3H}V' \quad (17)$$

Second,

$$\epsilon \equiv \frac{m_{Pl}^2}{16\pi} \left(\frac{V'}{V}\right)^2 \ll 1 \quad (18)$$

which means that the inflationary requirement  $\dot{\phi}^2 < V$  is well satisfied and

$$H^2 \simeq \frac{1}{3} \frac{8\pi}{m_{Pl}^2} V \quad (19)$$

These two conditions imply that  $H$  is slowly varying, and that the scale factor increases more or less exponentially,

$$a \propto e^{Ht} \quad (20)$$

The third condition that is usually satisfied is

$$|\eta| \ll 1 \quad (21)$$

where

$$\eta \equiv \frac{m_{Pl}^2}{8\pi} \frac{V''}{V} \quad (22)$$

It can be ‘derived’ from the other two by differentiating the approximation Eq. (17) for  $\dot{\phi}$  and noting that consistency with the exact expression Eq. (13) requires  $\ddot{\phi} \ll V'$  is satisfied. However there is no logical necessity for the derivative of an approximation to be itself a valid approximation, so this third condition is logically independent of the others. Conditions involving higher derivatives of  $V$  could be ‘derived’ by further differentiation, with the same caveat, but the two that we have given, involving only the first and second derivatives, are the ones needed to obtain the inflationary conditions for a scalar field. The

<sup>3</sup> An argument has been given for  $\Omega_0$  very close to 1 on the basis of effects on the cmb anisotropy from regions far outside the observable

in which they are satisfied and we are adopting that nomenclature here. Practically all of the usually considered models of inflation satisfy the slow-roll conditions more or less well.

It should be noted that the first slow-roll condition is on a quite different footing from the other two, being a statement about the *solution* of the field equation as opposed to a statement about the potential that defines this equation. What we are saying is that in the usually considered models one can show that the first condition is an attractor solution, in a regime typically characterized by the other two conditions, and that moreover reasonable initial conditions on  $\phi$  will ensure that this solution is achieved well before the observable universe leaves the horizon. It is important to remember that there are strong observational limits for the parameters previously introduced (e.g.  $\epsilon$ ,  $\eta$ ). For example [27] studied the possible contribution of a stochastic gravitational wave background to the anisotropy of the cosmic microwave background in cold and mixed dark matter (CDM and MDM) models. This contribution was tested against detections of CMB anisotropy at large and intermediate angular scales. The best fit parameters (i.e. those which maximize the likelihood) are (with 95% confidence)  $n_S = 1.23^{+0.17}_{-0.15}$  and

$$R(n_S) = \frac{C_2^T}{C_2^S} = \frac{29\epsilon}{\pi^2 f(n_S)} = 2.4^{+3.4}_{-2.2} \quad (23)$$

where

$$f(n_S) = \frac{\Gamma(3 - n_S)\Gamma(\frac{3 + n_S}{2})}{\Gamma^2(\frac{4 - n_S}{2})\Gamma(\frac{9 - n_S}{2})} \quad (24)$$

The previous constraint fixes the value of  $\epsilon$  as well that of  $\eta$

$$2\eta = n_S - 1 + 2\epsilon \quad (25)$$

They find that by including the possibility of such background in CMB data analysis it can drastically alter the conclusion on the remaining cosmological parameters. More stringent constraints on some of the previous parameters are given in section 1.12.

#### (h) Conclusions:

We have seen the possible values of  $\Omega$  using different methods. We have to add that Cosmologists are “attracted” by a value of  $\Omega_0 = 1$ . This value of  $\Omega$  is requested by inflationary theory. The previous data lead us to the following hypotheses:

i)  $\Omega_0 < 0.12$ ; in this case one can suppose that the universe is fundamentally made of baryonic matter (black holes; Jupiters; white dwarfs).

ii)  $\Omega_0 > 0.12$ ; in this case in order to have a flat universe, it is necessary a non-baryonic component.  $\Omega_b = 1$  is excluded by several reasons (see [28], [13]). The remaining possibilities are:

1) existence of a smooth component with  $\Omega = 0.8$ .

The test of a smooth component can be done with kinematic methods.

2) Existence of a cosmological term, absolutely smooth to whom correspond an energy density  $\rho_{vac} = \frac{\Lambda}{8\pi G}$ .

3) existence of non-baryonic matter: the universe is fundamentally done of particles (neutrinos, WIMPS (Weakly Interacting Massive Particles)).

4) A combination of 2) and 3).

Before going one, I want to recall that some authors ([29]; [30]; [31]) have assumed that we have a scant knowledge of physical laws. Sanders assumes that the gravitational

Milgrom assumes that the Newton law of gravitation is not valid when the gradient of the potential is small. In this case, the problem of the dynamics of clusters of galaxies is solved without introducing Dark Matter. In any case, the quoted assumptions have no general theory that can justify them.

### 1.2 Dark matter in particles

We know that if  $\Omega = 1$ , dark matter cannot be constituted exclusive of baryonic matter. The most widespread hypothesis is that dark matter is in form of particles. Several candidates exist: neutrinos, axions, neutralinos, photinos, gravitinos, etc. Interesting particles are usually grouped into three families:

HDM (Hot Dark Matter), CDM (Cold Dark Matter) and WDM (Warm Dark Matter). In order to understand this classification it is necessary to go back to the early phases of universe evolution. The history of the universe is characterized by long phases of local thermodynamic equilibrium (LTE) and by “deviation” by it: nucleosyntheses, baryogenesis, decoupling of species, etc. In the early universe, were present the particles that we know today and other particles predicted theoretically, but that have not been observed. Massive particles preserved the thermodynamic equilibrium concentration until the rate,  $\Gamma$ , of reactions and interactions that produced that concentration was larger than the expansion rate of the universe,  $H$ . When the condition  $\Gamma > H$  was no longer satisfied the reactions stopped and the abundance of the considered species remained constant at the value it had at time of freez-out,  $T_f$ , time at which  $\Gamma = H$ . If we indicate with  $Y = \frac{n}{s}$  the number of particles per unit comoving volume and we remember that  $n$  is the number density of species and  $s$  the entropy density, we obtain a contribution of the species to the actual density of the universe as  $\Omega h^2 = 0.28Y(T_f)(\frac{m}{eV})$  ([13]). At time  $T_f$ , particles could be relativistic or non-relativistic. Relativistic particles are today indicated with the term hot cosmic relics, HDM, while non-relativistic particles are named cold cosmic relics, CDM. There is an intermediate case, that of warm relics, WDM.

An example of HDM are massive neutrinos. Possible masses for these neutrinos are:

$$25\text{ev} \leq m_\nu \leq 100\text{ev} \quad (26)$$

([1]) and

$$m_\nu \geq \begin{cases} 4.9 - 1.3\text{Gev} & \text{for Maiorana's neutrinos} \\ 1.3 - 4.2\text{Gev} & \text{for Dirac's neutrinos} \end{cases} \quad (27)$$

([32]).

There are confirmed experimental evidence of the existence of massive neutrinos. In 1980, [33] announced the detection of an electronic antineutrino with mass 30 eV, by means of the shape of the electron energy spectrum in the  $\beta$  decay of tritium ([34]). Experiments (Super-Kamiokande, SNOW) have obtained some evidence of non-zero mass from neutrino oscillations. This yields a difference of square masses of order  $10^{-3}$  eV, and a mass of 0.05 eV (in the simplest case) (see [35]).

Among typical examples of CDM we have WIMPS and in particular axions and neutralinos (SUSY particle). This particle was postulated in order to solve the strong CP problem in nuclear physics. This problem arises from the fact that some interactions violate the parity, P, time inversion, T, and CP. If these are not eliminated, they give rise

limits ([13]). The solution to the problem was proposed by Peccei-Quinn in 1977 ([36]) in terms of a spontaneous symmetry breaking scheme. To this symmetry breaking should be associated a Nambu-Goldstone boson: the axion. The axion mass ranges between  $10^{-12} \text{ev} - 1 \text{Gev}$ . In cosmology there are two ranges of interest:  $10^{-6} \text{ev} \leq m_a \leq 10^{-3} \text{ev}$ ;  $3 \text{ev} \leq m_a \leq 8 \text{ev}$ . Axion production in the quoted range can originate due to a series of astrophysical processes ([13]) and several are the ways these particles can be detected. Nevertheless the effort of researchers especially in USA, Japan and Italy, axions remain hypothetical particles. They are in any case the most important CDM candidates.

In the following, I am going to speak about the basic ideas of structure formation. I shall write about density perturbations, their spectrum and evolution, about correlation functions and their time evolution, etc.

### 1.3 Origin of structures

Observing our universe, we notice a clear evidence of inhomogeneity when we consider small scales (Mpcs). In clusters density reaches values of  $10^3$  times larger than the average density, and in galaxies it has values  $10^5$  larger than the average density ([13]). If we consider scales larger than  $10^2$  Mpcs universe appears isotropic as it is observed in the radio-galaxies counts, in CMBR, in the X background ([11]). The isotropy at the decoupling time,  $t_{dec}$ , at which matter and radiation decoupled, universe was very homogeneous, as showed by the simple relation:

$$\frac{\delta\rho}{\rho} = \text{const} \frac{\delta T}{T} \quad (28)$$

([13])<sup>4</sup>. The difference between the actual universe and that at decoupling is evident. The transformation between a highly homogeneous universe, at early times, to an highly local non homogeneous one, can be explained supposing that at  $t_{dec}$  were present small inhomogeneities which grow up because of the gravitational instability mechanism ([37]). Events leading to structure formation can be enumerated as follows:

- (a) Origin of quantum fluctuations at Planck epoch.
- (b) Fluctuations enter the horizon and they grow linearly till recombination.
- (c) Perturbations grow up in a different way for HDM and CDM in the post-recombination phase, till they reach the non-linear phase.
- (d) Collapse and structure formation.

Before  $t_{dec}$  inhomogeneities in baryonic components could not grow because photons and baryons were strictly coupled. This problem was not present for the CDM component. Then CDM perturbations started to grow up before those in the baryonic component when universe was matter dominated. The epoch  $t_{eq} \approx 4.4 * 10^{10} (\Omega_0 h^2)^{-2} \text{sec}$ , at which matter and radiation density are almost equal, can be considered as the epoch at which structures started to form. The study of structure formation is fundamentally an initial value problem. Data necessary for starting this study are:

- 1) Value of  $\Omega_0$ . In CDM models the value chosen for this parameter is 1, in conformity with inflationary theory predictions.
- 2) The values of  $\Omega_i$  for the different components in the universe. For example in the case of baryons, nucleosynthesis

gives us the limit  $0.014 \leq \Omega_b \leq 0.15$  while  $\Omega_{WIMPS} \approx 0.9$ . 3) The perturbation spectrum and the nature of perturbations (adiabatic or isocurvature). The spectrum generally used is that of Harrison-Zeldovich:  $P(k) = Ak^n$  with  $n = 1$ . The perturbation more used are adiabatic or curvature. This choice is dictated from the comparison between theory and observations of CMBR anisotropy.

### 1.4 The spectrum of density perturbation

In order to study the distribution of matter density in the universe it is generally assumed that this distribution is given by the superposition of plane waves independently evolving, at least until they are in the linear regime (this means till the overdensity  $\delta = \frac{\rho - \bar{\rho}}{\bar{\rho}} \ll 1$ ). Let we divide universe in cells of volume  $V_u$  and let we impose periodic conditions on the surfaces. If we indicate with  $\bar{\rho}$  the average density in the volume and with  $\rho(\mathbf{r})$  the density in  $\mathbf{r}$ , it is possible to define the density contrast as:

$$\delta(\mathbf{r}) = \frac{\rho(\mathbf{r}) - \bar{\rho}}{\bar{\rho}} \quad (29)$$

This quantity can be developed in Fourier series:

$$\delta(\mathbf{r}) = \sum_{\mathbf{k}} \delta_{\mathbf{k}} \exp(i\mathbf{k}\mathbf{r}) = \sum_{\mathbf{k}} \delta_{\mathbf{k}} \exp(-i\mathbf{k}\mathbf{r}) \quad (30)$$

([13]), where  $k_x = \frac{2\pi n_x}{l}$  (and similar conditions for the other components) and for the periodicity condition  $\delta(x, y, L) = \delta(x, y, 0)$  (and similar conditions for the other components). Fourier coefficients  $\delta_{\mathbf{k}}$  are complex quantities given by:

$$\delta_{\mathbf{k}} = \frac{1}{V_u} \int_{V_u} \delta(\mathbf{r}) \exp(-i\mathbf{k}\mathbf{r}) d\mathbf{r} \quad (31)$$

For mass conservation in  $V_u$  we have also  $\delta_{\mathbf{k}=0} = 0$  while for reality of  $\delta(\mathbf{r})$ ,  $\delta_{\mathbf{k}}^* = \delta_{-\mathbf{k}}$ . If we consider  $n$  volumes,  $V_u$ , we have the problem of determining the distribution of Fourier coefficients  $\delta_{\mathbf{k}}$  and that of  $|\delta|$ . We know that the coefficients are complex quantities and then  $\delta_{\mathbf{k}} = |\delta_{\mathbf{k}}| \exp(i\theta_{\mathbf{k}})$ . If we suppose that phases are random, in the limit  $V_u \rightarrow \infty$  it is possible to show that we get  $|\delta|^2 = \sum_{\mathbf{k}} |\delta_{\mathbf{k}}|^2$ . The Central limit theorem leads us to conclude that the distribution for  $\delta$  is Gaussian:

$$P(\delta) \propto \exp\left(-\frac{\delta^2}{\sigma^2}\right) \quad (32)$$

([28]). The quantity  $\sigma$  that is present in Eq. (32) is the variance of the density field and is defined as:

$$\sigma^2 = \langle \delta^2 \rangle = \sum_{\mathbf{k}} \langle |\delta_{\mathbf{k}}|^2 \rangle = \frac{1}{V_u} \sum_{\mathbf{k}} \delta_{\mathbf{k}}^2 \quad (33)$$

This quantity characterizes the amplitude of the inhomogeneity of the density field. If  $V_u \rightarrow \infty$ , we obtain the more usual relation:

$$\sigma^2 = \frac{1}{(2\pi)^3} \int P(k) d^3k = \frac{1}{2\pi^2} \int P(k) k^2 dk \quad (34)$$

The term  $P(k) = \langle |\delta|^2 \rangle$  is called ‘‘Spectrum of perturbations’’. It is function only of  $k$  because the ensemble average in an isotropic universe depends only on  $r$ . A choice often made for the primordial spectrum is  $P(k) = Ak^n$  which in the case  $n = 1$  gives the scale invariant spectrum of Harrison-Zeldovich.

It can be defined as the joint probability of finding an overdensity  $\delta$  in two distinct points of space:

$$\xi(\mathbf{r}, t) = \langle \delta(\mathbf{r}, t) \delta(\mathbf{r} + \mathbf{x}, t) \rangle \quad (35)$$

([38]), where averages are averages on an ensemble obtained from several realizations of universe. Correlation function can be expressed as the joint probability of finding a galaxy in a volume  $\delta V_1$  and another in a volume  $\delta V_2$  separated by a distance  $r_{12}$ :

$$\delta^2 P = n_V^2 [1 + \xi(r_{12})] \delta V_1 \delta V_2 \quad (36)$$

where  $n_V$  is the average number of galaxies per unit volume. The concept of correlation function, given in this terms, can be enlarged to the case of three or more points.

Correlation functions have a fundamental role in the study of clustering of matter. If we want to use this function for a complete description of clustering, one needs to know the correlation functions of order larger than two ([39]). By means of correlation functions it is possible to study the evolution of clustering. The correlation functions are, in fact, connected one another by means of an infinite system of equations obtained from moments of Boltzmann equation which constitutes the BBGKY (Bogolyubov-Green-Kirkwood-Yvon) hierarchy ([40]). This hierarchy can be transformed into a closed system of equation using closure conditions. Solving the system one gets information on correlation functions.

In order to show the relation between perturbation spectrum and two-points correlation function, we introduce in Eq. (35), Eq. (30), recalling that  $\delta_{\mathbf{k}}^* = \delta(-\mathbf{k})$  and taking the limit  $V_u \rightarrow \infty$ , the average in the Eq. (35) can be expressed in terms of the integral:

$$\xi(\mathbf{r}) = \frac{1}{(2\pi)^3} \int |\delta(\mathbf{k})|^2 \exp(-i\mathbf{k}\mathbf{r}) d^3k \quad (37)$$

This result shows that the two-point correlation function is the Fourier transform of the spectrum. In an isotropic universe, it is  $|\mathbf{r}| = r$  and then  $|\mathbf{k}| = k$  and the spectrum can be obtained from an integral on  $|\mathbf{k}| = k$ . Then correlation function may be written as:

$$\xi(r) = \frac{1}{2\pi^2} \int k^2 P(k) \frac{\sin(kr)}{kr} dk \quad (38)$$

During the evolution of the universe and after perturbations enter the horizon, the spectrum is subject to modulations because of physical processes characteristic of the model itself (Silk damping ([41]) for acollisional components, free streaming for collisional particles, etc.). These effects are taken into account by means of the transfer function  $T(k; t)$  which connects the primordial spectrum  $P(k; t_p)$  at time  $t_p$  to the final time  $t_f$ :

$$P(k; t_f) = \left[ \frac{b(t_f)}{b(t_p)} \right]^2 T^2(k; t_f) P(k; t_p) \quad (39)$$

where  $b(t)$  is the law of grow of perturbations, in the linear regime. In the case of CDM models the transfer function is:

$$T(k) = \left\{ 1 + [ak + (bk)^{1.5} + (ck)^2]^\nu \right\}^{-\frac{1}{\nu}} \quad (40)$$

([42]), where  $a = 6.4(\Omega h^2)^{-1} Mpc$ ;  $b = 3.0(\Omega h^2)^{-1} Mpc$ ;  $c = 1.7(\Omega h^2)^{-1} Mpc$ ;  $\nu = 1.13$ . It is interesting to note that Eq. (32) is valid only if  $\sigma \ll 1$ , since  $|\delta| \leq 1$ . This implies than

certain point modes are no longer independent and start to couple giving rise to non-linear effects that change the spectrum and correlation function ([43]). There are also some theories (e.g., cosmic strings ([44])) in which even in the linear regime perturbations are not Gaussian.

### 1.5 Curvature and isocurvature perturbations

The study of the evolution of density perturbations can be divided into two phases:

1) perturbations are outside the horizon, in other terms they have a scale  $\lambda$  larger than Hubble radius  $r_H = ct$  or  $\lambda \geq H^{-1}$ ;

2) perturbations are inside the horizon,  $\lambda \leq H^{-1}$ .

In studying the first case it is necessary to use general relativity and one can demonstrate that two different kinds of fluctuations exist: curvature or adiabatic (motivated by the simplest models of inflation) and isocurvature or isothermal. Curvature fluctuations are characterized by a fluctuation in energy density or in space curvature. For them, we can write:

$$\frac{\delta S}{S} = \frac{3}{4} \frac{\delta \rho_r}{\rho_r} - \frac{\delta \rho_m}{\rho_m} = 3 \frac{\delta T}{T} - \frac{\delta \rho_m}{\rho_m} = 0 \quad (41)$$

([28]), where with m has been indicated the matter component, with r radiation, with S entropy and with T temperature. Last equation explains why these fluctuations are named adiabatic, since for them the entropy variation is zero.

Isocurvature or isothermal perturbations are not characterized by fluctuations in the curvature of the metric, but they are fluctuations in the local equation of state of universe and in agreement with the name it results  $\delta T = 0$ . Until fluctuations of isocurvature are not inside the horizon, the causality principle does not permit a redistribution of energy density. This is possible only when perturbations enter the Horizon and isocurvature perturbations can be converted into perturbations in the energy density. As a consequence, the distinction between those two kinds of perturbations is no longer meaningful after them enter the horizon ([45]; [46]). The origin of curvature perturbations may be explained inside inflationary models or assuming that they are initially present as perturbations of the metric. Isocurvature fluctuations may be always produced in inflationary scenarios from fluctuations in the density number of barions or axions ([28], [13]).

### 1.6 Perturbations evolution

Density perturbations in the components of the universe evolve with time. In order to get the evolution equations for  $\delta$  in Newtonian regime, it is possible to use several models. In our model, we assume that gravitation dominates on the other interactions and that particles (representing galaxies, etc.) move collisionless in the potential  $\phi$  of a smooth density function ([38]). The distribution function of particles for position and momentum is given by:

$$dN = f(\mathbf{x}, \mathbf{p}, t) d^3x d^3p \quad (42)$$

and density:

$$\rho(\mathbf{x}, t) = m a^{-3} \int d^3p f(\mathbf{x}, \mathbf{p}, t) = \rho_b [1 + \delta(\mathbf{x}, t)] \quad (43)$$

where  $m$  is the mass of a particle and  $\rho_b$  the background density. Applying Liouville theorem to the probability density on a limited region of phase-space of the system we have that  $f$  verifies the equation:

The distribution function  $f$  that appears in the previous equations cannot be obtained from observations. It is possible to measure moments of  $f$  (density, average velocity, etc.). We want now to obtain the evolution equations for  $\delta$ . For this reason, we start integrating Eq. (44) on  $\mathbf{p}$  and after using Eq. (43), we get:

$$a^3 \rho_b \frac{\partial \delta}{\partial t} + \frac{1}{a^2} \nabla \int \mathbf{p} f d^3 p = 0 \quad (45)$$

If we define velocity as:

$$\mathbf{v} = \frac{\int \frac{\mathbf{p}}{ma} f d^3 p}{\int f d^3 p} \quad (46)$$

and introduce it in Eq. (45) we get:

$$\rho_b \frac{\partial \delta}{\partial t} + \frac{1}{a} \nabla (\rho \mathbf{v}) = 0 \quad (47)$$

We can now multiply Eq. (44) for  $\mathbf{p}$  and integrate it on the momentum:

$$\frac{\partial}{\partial t} \int p_\alpha f d^3 p + \frac{1}{ma^2} \partial_\beta \int p_\alpha p_\beta f d^3 p + a^3 \rho(\mathbf{x}, t) \phi_{,\alpha} = 0 \quad (48)$$

this last in Eq. (45) leaves us with:

$$\frac{\partial^2 \delta}{\partial t^2} + 2 \frac{\dot{a}}{a} \frac{\partial \delta}{\partial t} = \frac{1}{a^2} \nabla [(1 + \delta) \nabla \phi] + \frac{1}{\rho_b m a^7} \partial_\alpha \partial_\beta \int p_\alpha p_\beta \phi d^3 p \quad (49)$$

and finally using

$$\langle v_\alpha v_\beta \rangle = \frac{\int f p_\alpha p_\beta d^3 p}{ma^2 \int f d^3 p} \quad (50)$$

the equation for the evolution of overdensity becomes:

$$\frac{\partial^2 \delta}{\partial t^2} + 2 \frac{\dot{a}}{a} \frac{\partial \delta}{\partial t} = \frac{1}{a^2} \nabla [(1 + \delta) \nabla \phi] + \frac{1}{a^2} \partial_\alpha \partial_\beta [(1 + \delta) \langle v^\alpha v^\beta \rangle] \quad (51)$$

([38]). The term  $\langle v_\alpha v_\beta \rangle$  is the tensor of anisotropy of peculiar velocity. This is present in the gradient and then it behaves as a pressure force. If we consider an isolated and spherical perturbation, it is possible to assume that initial asymmetries does not grow up and so we can suppose, in this hypothesis that  $\langle v_\alpha v_\beta \rangle = 0$ . In this case and with the linearity assumption  $\delta \ll 1$  we have:

$$\frac{\partial^2 \delta}{\partial t^2} + 2 \frac{\dot{a}}{a} \frac{\partial \delta}{\partial t} = 4\pi G \rho_b \delta \quad (52)$$

This equation in an Einstein-de Sitter universe ( $\Omega = 1$ ,  $\Lambda = 0$ ) has the solutions:

$$\delta_+ = A_+(\mathbf{x}) t^{\frac{2}{3}} \quad \delta_-(\mathbf{x}, t) = A_-(\mathbf{x}) t^{-1} \quad (53)$$

The perturbation is then done of two parts: a growing one, becoming more and more important with time, and a decaying one becoming negligible with increasing time, with respect to the growing one.

In the case of open models with no cosmological constant:  $\Omega < 1$ ,  $\Lambda = 0$ , we can write:

$$\frac{\dot{a}^2}{a^2} = \frac{8}{3} \pi G \bar{\rho} (1 + (\Omega_0^{-1} - 1) a), \quad (54)$$

$$a(\eta) = \frac{\Omega_0}{2(1 - \Omega_0)} (\cosh \eta - 1) \quad (55)$$

$$t(\eta) = \frac{\Omega_0}{2H_0(1 - \Omega_0)^{3/2}} (\sinh \eta - \eta).$$

In the case of flat models with positive cosmological constant:  $\Omega < 1$ ,  $\Lambda \neq 0$ ,  $\Omega + \Lambda/3H_0^2 = 1$ , we can write:

$$\frac{\dot{a}^2}{a^2} = \frac{8}{3} \pi G \bar{\rho} (1 + (\Omega_0^{-1} - 1) a^3), \quad (56)$$

$$a(t) = (\Omega_0^{-1} - 1)^{-1/3} \sinh^{2/3} \left( \frac{3}{2} \sqrt{\frac{\Lambda}{3}} t \right). \quad (57)$$

Before concluding this section, we want to find an expression for the velocity field in the linear regime. Using the equation of motion  $\mathbf{p} = ma^2 \dot{\mathbf{x}}$ ,  $\frac{d\mathbf{p}}{dt} = -m \nabla \phi$  and the proper velocity of a particle,  $v = a \dot{\mathbf{x}}$ , verify the equation:

$$\frac{d\mathbf{v}}{dt} + \mathbf{v} \frac{\dot{a}}{a} = -\frac{\nabla \phi}{a} = G \rho_b a \int d^3 x \delta(\mathbf{x}, t) \frac{\mathbf{x} - \mathbf{x}'}{|\mathbf{x} - \mathbf{x}'|} \quad (58)$$

Supposing that  $\mathbf{v}$  is a similar solution for the density,  $\mathbf{v} = \mathbf{V}_+(\mathbf{x}, t) t^p$ , we get:

$$v^\alpha = \frac{H a}{4\pi} \frac{\partial}{\partial x^\alpha} \int d^3 x' \frac{\delta(\mathbf{x}', t)}{|\mathbf{x}' - \mathbf{x}|} \quad (59)$$

([38]). This solution is valid just as that for  $\delta$  in the linear regime. At time  $t = t_0$  this regime is valid on scales larger than  $8h^{-1} \text{Mpc}$ .

### 1.7 Non-linear phase

Linear evolution is valid only if  $\delta \ll 1$  or similarly, if the mass variance,  $\sigma$ , is much less than unity. When this condition is no longer verified (e.g., if we consider scales smaller than  $8h^{-1} \text{Mpc}$ ), it is necessary to develop a non-linear theory. In regions smaller than  $8h^{-1} \text{Mpc}$  galaxies are not a Poisson distribution but they tend to cluster. If one wants to study the properties of galactic structures or clusters of galaxies, it is necessary to introduce a non-linear theory of clustering. A theory of this last item is too complicated to be developed in a purely theoretical fashion. The problem can be faced assuming certain approximations that simplifies it ([47]) or as often it is done, by using N-Body simulations of the interesting system. The approximations are often used to furnish the initial data to simulations. In the simulations, a large number of particles are randomly distributed in a sphere, in the points of a cubic grid, in order to eliminate small scale noise. The initial spectrum is obtained perturbing the initial positions by means of a superposition of plane waves having random distributed phases and wave vector ([48]). Obviously, the universe is considered in expansion (or comoving coordinates are used), and then the equation of motion of particles are numerically solved. For what concerns the analytical approximations one of the most used is that of [47]. This gives a solution to the problem of the grow of perturbations in an universe with  $p = 0$  not only in the linear regime but even in the mildly non-linear regime. In this approximation, one supposes to have particles with initial position given in Lagrangian coordinates  $\mathbf{q}$ . The positions of particles, at a given time  $t$ , are given by:



where  $\mathbf{x}$  indicates the Eulerian coordinates,  $\mathbf{p}(\mathbf{q})$  describes the initial density fluctuations and  $b(t)$  describes their growth in the linear phase and it satisfies the equation:

$$\frac{d^2b}{dt^2} + 2a^{-1}\frac{db}{dt}\frac{da}{dt} = 4\pi G\rho b \quad (61)$$

The equation of motion of particles, according to the quoted approximation, is given by:

$$\mathbf{v} = \dot{a}\mathbf{q} + \dot{b}\mathbf{p}(\mathbf{q}) \quad (62)$$

The peculiar velocity of particles is given by:

$$\mathbf{u} = \frac{d\mathbf{x}}{dt} = \frac{db}{dt}\mathbf{p}(\mathbf{q}) \quad (63)$$

while the density of the perturbed system is given by:

$$\rho(\mathbf{q}, t) = \bar{\rho} \left| \frac{\partial q_j}{\partial x_k} \right| = \bar{\rho} \left| \delta_{jk} + b(t) \frac{\partial p_k}{\partial q_j} \right|^{-1} \quad (64)$$

Developing the Jacobian present in Eq. (64) at first order in  $b(t)\mathbf{p}(\mathbf{q})$ , one obtains:

$$\frac{\delta\rho}{\bar{\rho}} \approx -b(t) \nabla_{\mathbf{q}} \mathbf{p}(\mathbf{q}) \quad (65)$$

This equation can be re-written, separating the space and time dependence, as in the equation for  $\mathbf{u}$ , and writing:

$$b(t) = t^{\frac{2}{3}} \quad \mathbf{p}(\mathbf{q}) = \sum_{\mathbf{k}} i \frac{\mathbf{k}}{|\mathbf{k}|^2} A_{\mathbf{k}} \exp(i\mathbf{k}\mathbf{q}) \quad (66)$$

in the form:

$$\frac{\delta\rho}{\bar{\rho}} = \sum_{\mathbf{k}} A_{\mathbf{k}} t^{\frac{2}{3}} \exp(i\mathbf{k}\mathbf{q}) \quad (67)$$

([28]), that leads us back to the linear theory. In other words, Zel'dovich approximation is able to reproduce the linear theory, and is also able to give a good approximation in regions with  $\frac{\delta\rho}{\bar{\rho}} \gg 1$ . Using the expression for  $p(q)$ , the Jacobian in Eq. (64) is a real matrix and symmetric that can be diagonalized. With this  $p(q)$  the perturbed density can be written as:

$$\rho(\mathbf{q}, t) = \frac{\bar{\rho}}{(1 - b(t)\lambda_1(q))(1 - b(t)\lambda_2(q))(1 - b(t)\lambda_3(q))} \quad (68)$$

where  $\lambda_1, \lambda_2, \lambda_3$  are the three eigenvalues of the Jacobian, describing the expansion and contraction of mass along the principal axes. From the structure of the last equation, we notice that in regions of high density Eq. (68) becomes infinite and the structure of collapse in a pancake, in a filamentary structure or in a node, according to values of eigenvalues. Some N-body simulations ([49]) tried to verify the prediction of Zel'dovich approximation, using initial conditions generated using a spectrum with a cut-off at low frequencies. The results showed a good agreement between theory and simulations, for the initial phases of the evolution ( $a(t) = 3.6$ ). Going on, the approximation is no more valid starting from the time of shell-crossing. After shell-crossing, particles do not oscillate any longer around the structure but they pass through it making it vanish. This problem has been partly solved supposing that particles, before reaching the singularity they sticks the one on the other, due to a dissipative term that simulates gravity and then collects on the forming structure. This model is known as “adesion-model” ([50]).

Summarizing, Zel'dovich approximation gives a description of the transition between linear and non-linear phase. It is a good approximation for the initial phases of the evolution.

## 1.8 Quasi-linear regime

We have seen in the previous section that in the case of regions of dimension smaller than  $8h^{-1}Mpc$ , the linear theory is no more a good approximation and a new theory is needed or N-body simulations. Non-linear theory is able to calculate quantities as the formation redshift of a given class of objects as galaxies and clusters, the number of bound objects having masses larger than a given one, the average virial velocity and the correlation function. It is possible to get an estimate of the given quantities as that of other not cited, using an intermediate theory between the linear and non-linear theory: the quasi-linear theory. This last is obtained adding to the linear theory a model of gravitational collapse, just as the spherical collapse model. Important results that the theory gives is the bottom-up formation of structures (in the CDM model). Other important results are obtained if we identify density peaks in linear regime with sites of structure formation. Two important papers in the development of this theory are [51] and that of [52]. This last paper is an application of the ideas of the quasi-linear theory to the CDM model. The principles of this approach are the following:

- Regions of mass larger than  $M$  that collapsed can be identified with regions where the density contrast evolved according to linear regime,  $\delta(M, x)$ , has a value larger than a threshold,  $\delta_c$ .
- After collapse regions does not fragment.

The major drawbacks of the theory, as described in [52] are fundamentally the fact that the estimates that can be obtained by means of this theory depends on the threshold  $\delta_c$ , on the ratio between the filtering mass and that of objects and from other parameters. Nevertheless, this theory has helped cosmologists in obtaining estimate of important quantities as those previously quoted, and at same time give evidences that leads to exclude very low values for spectrum normalization.

## 1.9 Spherical Collapse

Spherical symmetry is one of the few cases in which gravitational collapse can be solved exactly ([53]; [38]). In fact, as a consequence of Birkhoff's theorem, a spherical perturbation evolves as a FRW Universe with density equal to the mean density inside the perturbation.

The simplest spherical perturbation is the top-hat one, i.e. a constant overdensity  $\delta$  inside a sphere of radius  $R$ ; to avoid a feedback reaction on the background model, the overdensity has to be surrounded by a spherical underdense shell, such to make the total perturbation vanish. The evolution of the radius of the perturbation is then given by a Friedmann equation.

The evolution of a spherical perturbation depends only on its initial overdensity. In an Einstein-de Sitter background, any spherical overdensity reaches a singularity (collapse) at a final time:

$$t_c = \frac{3\pi}{2} \left( \frac{5}{3} \delta(t_i) \right)^{-3/2} t_i. \quad (69)$$

By that time its linear density contrast reaches the value:

$$\delta_c = 1.686$$

In an open Universe not any overdensity is going to collapse: the initial density contrast has to be such that the total density inside the perturbation overcomes the critical density. This can be quantified (not exactly but very accurately) as follows: the growing mode saturates at  $b(t) = 5/2(\Omega_0^{-1} - 1)$ , so that a perturbation ought to satisfy  $\delta_l > 1.69 \cdot 2(\Omega_0^{-1} - 1)/5$  to be able to collapse.

Of course, collapse to a singularity is not what really happens in reality. It is typically supposed that the structure reaches virial equilibrium at that time. In this case, arguments based on the virial theorem and on energy conservation show that the structure reaches a radius equal to half its maximum expansion radius, and a density contrast of about 178. In the subsequent evolution the radius and the physical density of the virialized structure remains constant, and its density contrast grows with time, as the background density decays. Similarly, structures which collapse before are denser than the ones which collapse later.

Spherical collapse is not a realistic description of the formation of real structures; however, it has been shown (see [54] for a rigorous proof or [55], [56]) that high peaks ( $> 2\sigma$ ) follow spherical collapse, at least in the first phases of their evolution. However, a small systematic departure from spherical collapse can change the statistical properties of collapse times.

Spherical collapse can describe the evolution of underdensities. A spherical underdensity is not able to collapse (unless the Universe is closed!), but behaves as an open Universe, always expanding unless its borders collide with neighboring regions. At variance with overdensities, underdensities tend to be more spherical as they evolve, so that the spherical model provides a very good approximation for their evolution.

### 1.9.1 Improvements to the Spherical Collapse model

Several years ago it was realized that the density field distributions around the density peaks, which eventually will give birth to galaxies and clusters, depart from spherical symmetry and from the average density profile, producing important consequences on collapse dynamics and formation of protostructures ([57]; [58]; [59]; [60], [61]; [62]). A fundamental role in this context is played by the joint action of tidal torques (coupling shells of matter which are accreted around a density peak and neighboring protostructures ([58]; [59])), and by dynamical friction ([63]; [60], [61], [64]).

According to the previrialization conjecture ([65], [62]), initial asphericities and tidal interactions between neighboring density fluctuations induce significant non-radial motions which oppose the collapse. This means that virialized clumps form later, with respect to the predictions of the linear perturbation theory or the spherical collapse model (hereafter SM), and that the initial density contrast, needed to obtain a given final density contrast, must be larger than that for an isolated spherical fluctuation. This kind of conclusion was supported by [66], [67], [68], [69] and [70].

In particular [66] and [67] pointed out that non-radial motions would slow the rate of growth of the density contrast by lowering the peculiar velocity and suppress collapse once the system detaches from general expansion. [68] gave examples of the growth of non-radial motions in N-body simulations. Arguments based on a numerical least-action method lead [62] to the conclusion that irregularities in the mass distribution, together with external tides, induce non-radial motions that slow down the collapse. [70] used N-body simulations to show that the collapse of a perturbation

the slope of the initial power spectrum is  $n > -1$ , non-linear tidal interactions slow down the growth of density fluctuations and the magnitude of the effect increases when  $n$  is increased.

Opposite conclusions were obtained by [71], [72], [73], [74]. In particular [71], using the quasi-linear (QL) approximation ([47]) showed that the shear affects the dynamics of collapsing objects and it leads to infall velocities that are larger than in the case of non-shearing ones. Bertschinger & Jain ([73]) put this result in theorem form, according to which spherical perturbations are the slowest in collapsing. Bartelmann et al. (1993) argued that the collapse does not start from a comoving motion of the perturbation, but that the continuity equation requires an initial velocity perturbation directly related to the density perturbation. The effect is that collapse proceeds faster than in the case where the initial velocity perturbation is set equal to zero and the collapse timescale is shortened. The N-body simulations by [72] did not reproduce previrialization effect, but the reason is due to the fact that they assumed an  $n = -1$  spectrum, differently from the  $n = 0$  one used by [62] that reproduced the effect. If  $n < -1$  the peculiar gravitational acceleration,  $g \propto R^{-(n+1)/2}$ , diverges at large  $R$  and the gravitational acceleration moves the fluid more or less uniformly, generating bulk flows rather than shearing motions. Therefore, its collapse will be similar to that of an isolated spherical clump. If  $n > -1$ , the dominant sources of acceleration are local, small-scale inhomogeneities and tidal effects will tend to generate non-radial motions and resist gravitational collapse. In a more recent paper, [75] have proposed some analytic prescriptions to compute the collapse time along the second and the third principal axes of an ellipsoid, by means of the 'fuzzy' threshold approach. They pointed out that the formation of real virialized clumps must correspond to the third axis collapse and that the collapse along this axis is slowed down by the effect of the shear rather than be accelerated by it, in contrast to its effect on the first axis collapse. They concluded that spherical collapse is the fastest, in disagreement with Bertschinger & Jain's theorem. This result is in agreement with [62]. The quoted controversy was addressed by [76] who examined the evolution of non-spherical inhomogeneities in a Einstein-de Sitter universe, by numerically solving the equations of motion for the principal axes and the density of a dust ellipsoid. They showed that for lower values of  $\nu$  ( $\nu = 2$ ) the growth rate enhancement of the density contrast induced by the shear is counterbalanced by the effect of angular momentum acquisition. For  $\nu > 3$  the effect of angular momentum and shear reduces, and the evolution of perturbations tends to follow the behavior obtained in the SM. [77] studied the role of shear fields on the evolution of density perturbations by using an analytical approximate solution for the equations of motion of homogeneous ellipsoids embedded in a homogeneous background. The equations of motion of a homogeneous ellipsoid ([78]; [79] (hereafter WS)) were modified in order to take account of the tidal field, as done in [80] and then were integrated analytically, similar to what was done in WS. The density contrast at turn-around and the collapse velocity were found to be reduced with respect to that found by means of the SM. The reduction increases with increasing strength of the external tidal field and with increasing initial asymmetry of the ellipsoids.

The second physical effect with changes cluster collapse is dynamical friction. Former treatments of the dynamical friction effects on the structure of clusters of galaxies, considering only the component generated by the galactic

namical friction taking into account the effect of substructure, showing that dynamical friction delays the collapse of low- $\nu$  peaks inducing a bias of dynamical nature. Because of dynamical friction under-dense regions in clusters (the clusters outskirts) accrete less mass with respect to that accreted in absence of this dissipative effect and as a consequence over-dense regions are biased toward higher mass (AC). Dynamical friction and non-radial motions acts in a similar fashion: they delay the shell collapse consequently inducing a dynamical bias. Whenever efficient, these mechanisms will generate a physical selection of those peaks in the initial density field that eventually will give rise to the observed cosmic structures. As a consequence of dynamical friction and tidal torques, one expects changes in the threshold of collapse, the mass function and the correlation function.

In the next subsections, I shall study how the spherical collapse model is changed by the joint effect of dynamical friction, tidal torques and a non-zero cosmological constant.

### 1.9.2 Dynamical friction and structure formation

In a hierarchical structure formation model, the large scale cosmic environment can be represented as a collisionless medium made of a hierarchy of density fluctuations whose mass,  $M$ , is given by the mass function  $N(M, z)$ , where  $z$  is the redshift. In these models matter is concentrated in lumps, and the lumps into groups and so on. In such a material system, gravitational field can be decomposed into an average field,  $\mathbf{F}_0(r)$ , generated from the smoothed out distribution of mass, and a stochastic component,  $\mathbf{F}_{stoch}(r)$ , generated from the fluctuations in number of the field particles. The stochastic component of the gravitational field is specified assigning a probability density,  $W(\mathbf{F})$ , ([82]). In an infinite homogeneous unclustered system  $W(\mathbf{F})$  is given by Holtmark distribution ([82]) while in inhomogeneous and clustered systems  $W(\mathbf{F})$  is given by [83] and [84] respectively. The stochastic force,  $\mathbf{F}_{stoch}$ , in a self-gravitating system modifies the motion of particles as it is done by a frictional force. In fact a particle moving faster than its neighbors produces a deflection of their orbits in such a way that average density is greater in the direction opposite to that of traveling causing a slowing down in its motion. Following [82] method, the frictional force which is experienced by a body of mass  $M$  (galaxy), moving through a homogeneous and isotropic distribution of lighter particles of mass  $m$  (substructure), having a velocity distribution  $n(v)$  is given by:

$$M \frac{d\mathbf{v}}{dt} = -4\pi G^2 M^2 n(v) \frac{\mathbf{v}}{v^3} \log \Lambda \rho \quad (71)$$

where  $\log \Lambda$  is the Coulomb logarithm,  $\rho$  the density of the field particles (substructure).

A more general formula is that given by [83] in the hypothesis that there are no correlations among random force and their derivatives:

$$\mathbf{F} = -\eta \mathbf{v} = -\frac{\int W(F) F^2 T(F) d^3 F}{2 \langle v^2 \rangle} \mathbf{v} \quad (72)$$

where  $\eta$  is the coefficient of dynamical friction,  $T(F)$  the average duration of a random force impulse,  $\langle v^2 \rangle$  the characteristic speed of a field particle having a distance  $r \simeq (\frac{GM}{F})^{1/2}$  from a test particle (galaxy). This formula is more general than Eq. (71) because the frictional force can be calculated also for inhomogeneous systems when  $W(F)$  is given. If the field particles are distributed homogeneously the dynamical friction force is given by:

([83]), where  $m_a$  and  $n_a$  are respectively the average mass and density of the field particles. Using virial theorem we also have:

$$\frac{\langle v^2 \rangle}{G m_a n_a^{1/3}} \simeq \frac{M_{tot}}{m} \frac{1}{n^{1/3} R_{sys}} \simeq N^{2/3} \quad (74)$$

where  $M_{tot}$  is the total mass of the system,  $R_{sys}$  its radius and  $N$  is the total number of field particles. The dynamical friction force can be written as follows:

$$F = -\eta v = -\frac{4.44 [G m_a n_{ac}]^{1/2}}{N} \log \left\{ 1.12 N^{2/3} \right\} \frac{v}{a^{3/2}} = -\epsilon_o \frac{v}{a^{3/2}} \quad (75)$$

where  $N = \frac{4\pi}{3} R_{sys}^3 n_a$  and  $n_{ac} = n_a \times a^3$  is the comoving number density of peaks of substructure of field particles. This last equation supposes that the field particles generating the stochastic field are virialized. This is justified by the previrialization hypothesis ([65]).

To calculate the dynamical evolution of the galactic component of the cluster it is necessary to calculate the number and average mass of the field particles generating the stochastic field.

The protocluster, before the ultimate collapse at  $z \simeq 0.02$ , is made of substructure having masses ranging from  $10^6 - 10^9 M_\odot$  and from galaxies. I suppose that the stochastic gravitational field is generated from that portion of substructure having a central height  $\nu$  larger than a critical threshold  $\nu_c$ . This latter quantity can be calculated (following AC) using the condition that the peak radius,  $r_{pk}(\nu \geq \nu_c)$ , is much less than the average peak separation  $n_a(\nu \geq \nu_c)^{-1/3}$ , where  $n_a$  is given by the formula of [52] for the upcrossing points:

$$n_{ac}(\nu \geq \nu_c) = \frac{\exp(\nu_c^2/2)}{(2\pi)^2} \left( \frac{\gamma}{R_*} \right)^3 [\nu_c^2 - 1 + \frac{4\sqrt{3}}{5\gamma^2(1 - 5\gamma^2/9)^{1/2}} \exp(-5\gamma^2\nu_c^2/18)] \quad (76)$$

where  $\gamma, R_*$  are parameters related to moments of the power spectrum ([52] Eq. 4.6A). The condition  $r_{pk}(\nu \geq \nu_c) < 0.1 n_a(\nu \geq \nu_c)^{-1/3}$  ensures that the peaks of substructure are point like. Using the radius for a peak:

$$r_{pk} = \sqrt{2} R_* \left[ \frac{1}{(1 + \nu \sigma_0)(\gamma^3 + (0.9/\nu)^{3/2})} \right]^{1/3} \quad (77)$$

(AC), I obtain a value of  $\nu_c = 1.3$  and then we have  $n_a(\nu \geq \nu_c) = 50.7 Mpc^{-3}$  ( $\gamma = 0.4$ ,  $R_* = 50 Kpc$ ) and  $m_a$  is given by:

$$m_a = \frac{1}{n_a(\nu \geq \nu_c)} \int_{\nu_c}^{\infty} m_{pk}(\nu) N_{pk}(\nu) d\nu = 10^9 M_\odot \quad (78)$$

(in accordance with the result of AC), where  $m_{pk}$  is given in [85] and  $N_{pk}$  is the average number density of peak ([52] Eq. 4.4). Galaxies and Clusters of galaxies are correlated systems whose autocorrelation function,  $\xi(r)$ , can be expressed, in a power law form ([38]; [86]; [87]; [88]; [89]). The description of dynamical friction in these systems need to use a distribution of the stochastic forces,  $W(F)$ , taking account of correlations. In this last case the coefficient of dynamical friction,  $\eta$ , may be calculated using the equation:

$$\eta = \int d^3 \mathbf{F} W(F) F^2 T(F) / (2 \langle v^2 \rangle) \quad (79)$$

and using [84] distribution:

where  $A_f$ , which is a linear integral function of the correlation function  $\xi(r)$ , is given in the quoted paper (Eq. 36).

### 1.9.3 Tidal torques and structure formation

The explanation of galaxies spins gain through tidal torques was pioneered by [90]. Peebles ([91]) performed the first detailed calculation of the acquisition of angular momentum in the early stages of protogalactic evolution. More recent analytic computations ([92], [71], [58]; [93]; [94]; [95] and numerical simulations ([96]) have re-investigated the role of tidal torques in originating galaxies angular momentum. One way to study the variation of angular momentum with radius in a galaxy is that followed by [58]. In this approach the protogalaxy is divided into a series of mass shells and the torque on each mass shell is computed separately. The density profile of each proto-structure is approximated by the superposition of a spherical profile,  $\delta(r)$ , and a random CDM distribution,  $\varepsilon(\mathbf{r})$ , which provides the quadrupole moment of the protogalaxy. As shown by [58] the net rms torque on a mass shell centered on the origin of internal radius  $r$  and thickness  $\delta r$  is given by:

$$\langle |\tau|^2 \rangle^{1/2} = \sqrt{30} \left( \frac{4\pi}{5} G \right) [\langle a_{2m}(r)^2 \rangle \langle q_{2m}(r)^2 \rangle - \langle a_{2m}(r) q_{2m}^*(r) \rangle^2]^{1/2} \quad (81)$$

where  $q_{lm}$ , the multipole moments of the shell and  $a_{lm}$ , the tidal moments, are given by:

$$\langle q_{2m}(r)^2 \rangle = \frac{r^4}{(2\pi)^3} M_{sh}^2 \int k^2 dk P(k) j_2(kr)^2 \quad (82)$$

$$\langle a_{2m}(r)^2 \rangle = \frac{2\rho_b^2 r^{-2}}{\pi} \int dk P(k) j_1(kr)^2 \quad (83)$$

$$\langle a_{2m}(r) q_{2m}^*(r) \rangle = \frac{r}{2\pi^2} \rho_b M_{sh} \int k dk P(k) j_1(kr) j_2(kr) \quad (84)$$

where  $M_{sh}$  is the mass of the shell,  $j_1(r)$  and  $j_2(r)$  are the spherical Bessel function of first and second order while the power spectrum  $P(k)$  is given by, [52] (equation (G3)):

$$T(k) = \frac{[\ln(1 + 2.34q)]}{2.34q} \cdot [1 + 3.89q + (16.1q)^2 + (5.46q)^3 + (6.71q)^4]^{-1} \quad (85)$$

(where  $q = \frac{k\theta^{1/2}}{\Omega_b h^2 M_{pc}^{-1}}$ . Here  $\theta = \rho_{er}/(1.686\rho_\gamma)$  represents the ratio of the energy density in relativistic particles to that in photons ( $\theta = 1$  corresponds to photons and three flavors of relativistic neutrinos). The power spectrum was normalized to reproduce the observed abundance of rich cluster of galaxies. Filtering the spectrum on cluster scales,  $R_f = 3h^{-1}Mpc$ , I have obtained the rms torque,  $\tau(r)$ , on a mass shell using Eq. (81) then I obtained the total specific angular momentum,  $h(r, \nu)$ , acquired during expansion integrating the torque over time ([58] Eq. 35):

$$h(r, \nu) = \frac{1}{3} \left( \frac{3}{4} \right)^{2/3} \frac{\tau_o t_o}{M_{sh}} \delta_o^{-5/2} \int_0^\pi \frac{(1 - \cos \theta)^3}{(\vartheta - \sin \vartheta)^{4/3}} \frac{f_2(\vartheta)}{f_1(\vartheta) - f_2(\vartheta) \frac{\delta_o}{\delta_o}} d\vartheta \quad (86)$$

the functions  $f_1(\vartheta)$ ,  $f_2(\vartheta)$  are given by [58] (Eq. 31) while the mean over-density inside the shell,  $\bar{\delta}(r)$ , is given by [58]:

where  $\delta(r) = \frac{\rho(r) - \rho_b}{\rho_b}$ . As showed by [58], the rms specific angular momentum,  $h(r, \nu)$ , increases with distance  $r$  while peaks of greater  $\nu$  acquire less angular momentum via tidal torques. This is the angular momentum-density anticorrelation showed by [71]. This effect arises because the angular momentum is proportional to the gain at turn around time,  $t_m$ , which in turn is proportional to  $\bar{\delta}(r, \nu)^{-\frac{3}{2}} \propto \nu^{-3/2}$ .

### 1.9.4 Modification of collapse

Tidal torques and dynamical friction acts in a similar fashion. As previously reported, AC calculated the effect of dynamical friction taking into account the effect of substructure, showing that dynamical friction delays the collapse of low- $\nu$  peaks inducing a bias of dynamical nature. Similarly non-radial motions would slow the rate of growth of the density contrast by lowering the peculiar velocity and suppress collapse once the system detaches from general expansion. In fact, in the central regions of a density peak ( $r \leq 0.5R_f$ ) the velocity dispersion attain nearly the same value while at larger radii ( $r \geq R_f$ ) the radial component is lower than the tangential component. This means that motions in the outer regions are predominantly non-radial and in these regions the fate of the infalling material could be influenced by the amount of tangential velocity relative to the radial one. This can be shown writing the equation of motion of a spherically symmetric mass distribution with density  $n(r)$  ([97]):

$$\frac{\partial}{\partial t} n \langle v_r \rangle + \frac{\partial}{\partial r} n \langle v_r^2 \rangle + (2 \langle v_r^2 \rangle - \langle v_\vartheta^2 \rangle) \frac{n}{r} + n(r) \frac{\partial}{\partial t} \langle v_r \rangle = 0 \quad (88)$$

where  $\langle v_r \rangle$  and  $\langle v_\vartheta \rangle$  are, respectively, the mean radial and tangential streaming velocity. Eq. (88) shows that high tangential velocity dispersion ( $\langle v_\vartheta^2 \rangle \geq 2 \langle v_r^2 \rangle$ ) may alter the infall pattern. The expected delay in the collapse of a perturbation, due to non-radial motions, dynamical friction and also taking account of a non-zero cosmological constant, may be calculated solving the equation for the radial acceleration ([81]; [60]; [61]; AC; [97]):

$$\frac{dv_r}{dt} = \frac{L^2(r, \nu)}{M^2 r^3} - g(r) - \eta \frac{dr}{dt} + \frac{\Lambda}{3} r \quad (89)$$

where  $L(r, \nu)$  is the angular momentum,  $g(r)$  the acceleration, and  $\Lambda$  the cosmological constant. Writing the proper radius of a shell in terms of the expansion parameter,  $a(r_i, t)$ :

$$r(r_i, t) = r_i a(r_i, t) \quad (90)$$

remembering that

$$M = \frac{4\pi}{3} \rho_b(r_i, t) a^3(r_i, t) r_i^3 \quad (91)$$

and that  $\rho_b = \frac{3H_0^2}{8\pi G}$ , where  $H_0$  is the Hubble constant and assuming that no shell crossing occurs so that the total mass inside each shell remains constant, that is:

$$\rho(r_i, t) = \frac{\rho_i(r_i, t)}{a^3(r_i, t)} \quad (92)$$

the Eq. (89) may be written as:

$$\frac{d^2 a}{dt^2} = -\frac{H^2(1 + \bar{\delta})}{2a^2} + \frac{4G^2 L^2}{H^4(1 + \bar{\delta})^2 r_i^{10} a^3} - \eta \frac{da}{dt} + \frac{\Lambda}{3} a \quad (93)$$

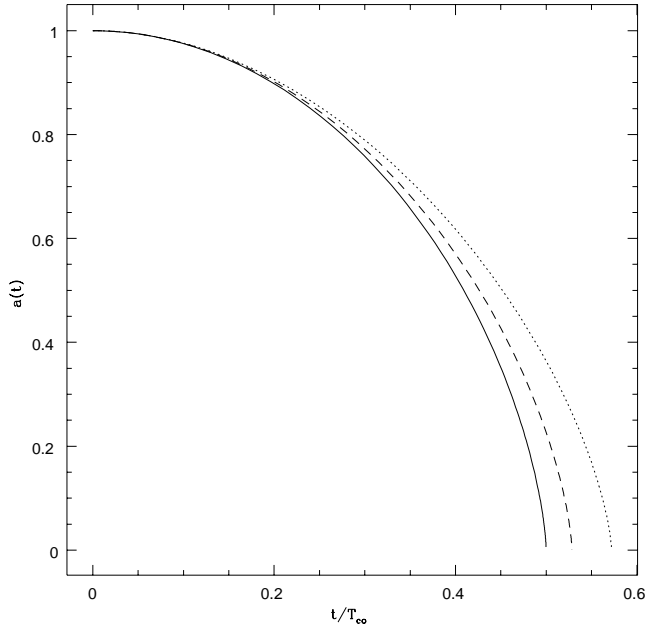


FIG. 1: The time evolution of the expansion parameter. The solid line is  $a(t)$  for the SM; the dashed line is  $a(t)$  taking account only dynamical friction; the dotted line is  $a(t)$  taking account of the cumulative effect of non-radial motions and dynamical friction in the case of a  $\nu = 2$  peak.

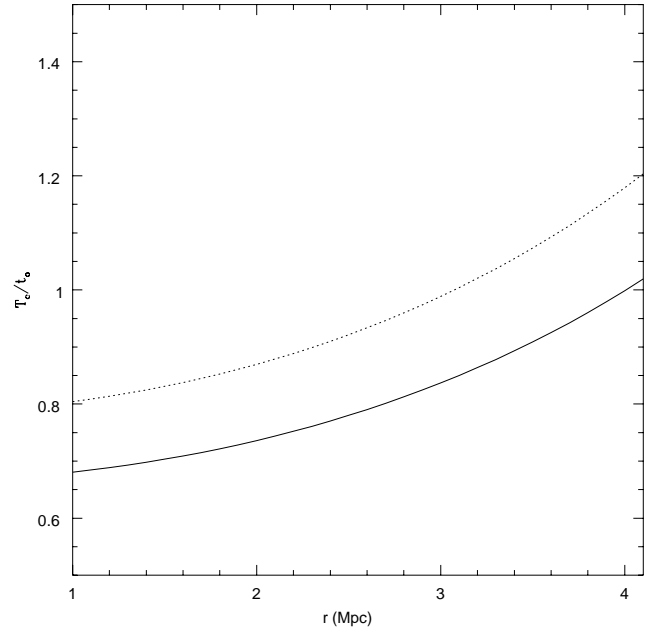
$h(r, \nu) = L(r, \nu)/M_{sh}$  found in Eq. (86), to obtain  $a(t)$  and the time of collapse,  $T_c(r, \nu)$ . As shown by [53], this last quantity in the case of a pure SM (namely when tidal torques, dynamical friction and cosmological constant are not taken into account) is given by:

$$T_{c0}(r, \nu) = \frac{\pi}{H_i [\bar{\delta}(r, \nu)]^{3/2}}^5 \quad (94)$$

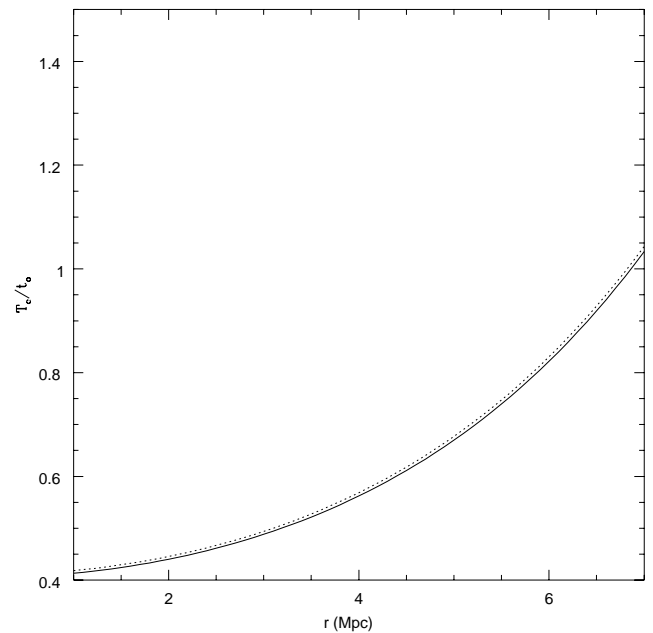
In Fig. 1, I show the effects of non-radial motions and dynamical friction separately, in the case of a  $\nu = 2$  peak. As displayed non-radial motions have a larger effect on the collapse delay with respect to dynamical friction. In Fig. 2, I compare the results for the time of collapse,  $T_c$ , for  $\nu = 2, 4$  with the time of collapse of the classical SM (Eq. 94). As shown the presence of non-radial motions produces an increase in the time of collapse of a spherical shell. The collapse delay is larger for low value of  $\nu$  and becomes negligible for  $\nu \geq 3$ . This result is in agreement with the angular momentum-density anticorrelation effect: density peaks having low value of  $\nu$  acquire a larger angular momentum than high  $\nu$  peaks and consequently the collapse is more delayed with respect to high  $\nu$  peaks.

Given  $T_c(r, \nu)$ , I also calculated the total mass gravitationally bound to the final non-linear configuration. There are at least two criteria to establish the bound region to a perturbation  $\delta(r)$ : a statistical one ([59]), and a dynamical one ([57], summarized in the following.

In biased galaxy formation theory structures form around the local maxima of the density field. Every density peak binds a mass  $M$  that can be calculated when we know the binding radius of the density peak. The radius of the bound



2a



2b

FIG. 2: Fig. 2a. The time of collapse of a shell of matter in units of the age of the universe  $t_0$  for  $\nu = 2$  (dotted line) compared with SM (solid line). Fig. 2b. The time of collapse of a shell of matter in units of the age of the universe  $t_0$  for  $\nu = 4$  (dotted line) compared with SM (solid line).

region for a chosen density profile  $\bar{\delta}(r)$  may be obtained in several ways. A first criterion is statistic. The binding radius of the region,  $r_b$ , is given by the solution of the equation:

$$\langle \bar{\delta}(r) \rangle = \langle (\bar{\delta} - \langle \bar{\delta} \rangle)^2 \rangle^{1/2} \quad (95)$$

([58]; [59]). At radius  $r \ll r_b$  the motion of particles is predominant toward the peak while when  $r \gg r_b$  the particle is not bound to the peak. Another criterion that can be used is dynamical. It supposes that the binding radius is given by the condition that a shell collapse in a time,  $T_c$ , smaller than the age of the universe  $t_0$ :

$$T_c(r) \leq t_0 \quad (96)$$

<sup>5</sup> As we told in the introduction, the inclusion of the peculiar velocity field changes the collapse as:  $H_i T_{c0} \simeq \frac{\pi}{(c\delta_i - \epsilon_i)^{3/2}}$  where  $c$  and  $\epsilon_i$

physics of the collapse process of a shell. For this reason I used it to calculate the binding radius. The time of collapse,  $T_c(r)$ , at radius  $r$  can be obtained solving numerically Eq. (93) for different values of  $\delta_i$ , the initial overdensity, from a given density profile  $\bar{\delta}(r)$ . I use the average density profile given by [52]:

$$\delta(r) = A \left\{ \frac{\nu \xi(r)}{\xi(0)^{1/2}} - \frac{\theta(\nu\gamma, \gamma)}{\gamma \xi(0)^{1/2} (1 - \gamma^2)} \left[ \gamma^2 \xi(r) + \frac{R_*^2 \nabla^2 \xi(r)}{3} \right] \right\} \quad (97)$$

where  $A$  is a constant given by the normalization of the perturbation spectrum,  $P(k)$ ,  $\nu = \frac{\delta_{co}}{\sigma(M)}$ , where  $\delta_{co} = 1.686$  is the critical threshold for a SM,  $\sigma(M)$  is the r.m.s. density fluctuation on the mass scale  $M$ ,  $\xi(r)$  is the correlation function of two points,  $\gamma$  and  $R_*$  two constants obtainable from the spectrum (see [52]) and finally  $\theta(\gamma\nu, \gamma)$  is a function given in the quoted paper (eq. 6.14). Given the average density profile the average density inside the radius  $r$  in a spherical perturbation is given by Eq. (87).

Finally, I calculated the binding radius,  $r_b(\nu)$ , for a SM, calculating  $T_{co}(r)$  by means of Eq. (94) and the density profile given in Eq. (97) and then applying the condition  $T_{co}(r) \leq t_o$ . I repeated the calculation for  $1.7 < \nu < 4$ . Then I repeated the calculation using  $T_c(r)$ , the collapse time that takes into account non-radial motions and dynamical friction. I found a relation between  $\nu$  and the mass of the cluster using the equation:  $M = \frac{4\pi}{3} r_b^3 \rho_b$ . The result is the plot in Fig. 3 for the binding radius  $r_b$  versus  $\nu$ .

In fig. 4, I compare the peak mass obtained from SM, using [57] criterion, with that obtained from the model taking into account non-radial motions, dynamical friction and  $\Lambda \neq 0$ . As shown for high values of  $\nu$  ( $\nu \geq 3$ ) the two models give the same result for the mass while for  $\nu < 3$  the effect of non-radial motions produces less bound mass with respect to SM. Decreasing the effect of non-radial motions produces a decrease in the bound mass.

The situation represented in the previous three figures may be summarized as follows: dynamical friction and non-radial motions delays the collapse of perturbations. Both effects act in the direction of delaying structure collapse, so that their effects add. The effects have a similar magnitude, but non-radial motions induce a slight larger delay in collapse. As a consequence of this delay of collapse the matter bound to structures is less than what expected in the case of SM.

### 1.9.5 The threshold of collapse $\delta_c$

In this section, I am going to show how dynamical friction and tidal fields influence the critical overdensity threshold for the collapse,  $\delta_c$ , which is not constant as in a SM but it depends on mass. An analytic determination of  $\delta_c(\nu)$  can be obtained following a technique similar to that used by [98].

Using Eq. (93) it is possible to obtain the value of the expansion parameter of the turn around epoch,  $a_{max}$ , which is characterized by the condition  $\frac{da}{dt} = 0$ . Using the relation between  $\nu$  and  $\delta_i$ , in linear theory ([38]), I find:

$$B(M) = \delta_c = \delta_{co} \left[ 1 + \int_{r_i}^{r_{ta}} \frac{r_{ta} L^2 \cdot dr}{GM^3 r^3} + \frac{\lambda_o}{1 - \mu(\delta)} + \Lambda \frac{r_{ta} r^2}{6GM} \right] \quad (98)$$

where  $\delta_{co} = 1.686$  is the critical threshold for SM,  $r_i$  is the initial radius,  $r_{ta}$  is the turn-around radius,  $\lambda_o = \epsilon_o T_{co}$  and  $\mu(\delta)$  is the dynamical friction coefficient. The coefficient  $\Lambda$  is the

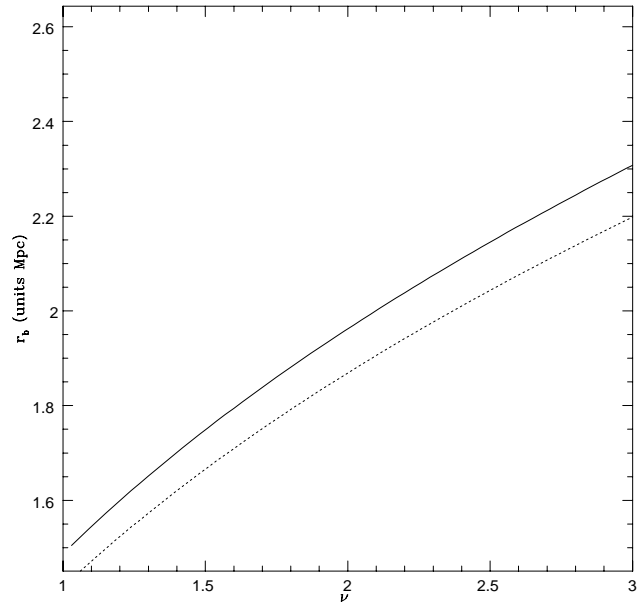


FIG. 3: Variation of the binding radius  $r_b$  with  $\nu$ . The solid line is the binding radius in the SM, while the dashed line is the same as in presence of non-radial motions dynamical friction and  $\Lambda \neq 0$ , for  $\nu = 2$ .

proto-structure during evolution that is calculated as shown in section 1.9.3. The result of the calculation is shown in Fig. 5, where I plot  $\delta_c(\nu)$  obtained by means of the model of the present paper together with that obtained by [100] (ST) using an ellipsoidal collapse model. The dashed line represents  $\delta_c(\nu)$  obtained with the present model, while the solid line that of ST. Both models show that the threshold for collapse decreases with mass and when  $\nu > 3$  the threshold assume the typical value of the SM. In other words, this means that, in order to form structure, more massive peaks must cross a lower threshold,  $\delta_c(\nu)$ , with respect to under-dense ones. At the same time, since the probability to find high peaks is larger in more dense regions, this means that, statistically, in order to form structure, peaks in more dense regions may have a lower value of the threshold,  $\delta_c(\nu)$ , with respect to those of under-dense regions. This is due to the fact that less massive objects are more influenced by external tides, and consequently they must be more overdense to collapse by a given time. In fact, the angular momentum acquired by a shell centered on a peak in the CDM density distribution is anti-correlated with density: high-density peaks acquire less angular momentum than low-density peaks ([71]; [58]; [59]). A larger amount of angular momentum acquired by low-density peaks (with respect to the high-density ones) implies that these peaks can more easily resist gravitational collapse and consequently it is more difficult for them to form structure. This is in agreement with [75], [62], which pointed out that the gravitational collapse is slowed down by the effect of the shear rather than fastened by it (as sustained by other authors). Therefore, on small scales, where the shear is statistically greater, structures need, on average, a higher density contrast to collapse. This results in a tendency for less dense regions to accrete less mass, with respect to a classical SM, inducing a *biasing* of over-dense regions towards higher mass.

### 1.10 Mass function

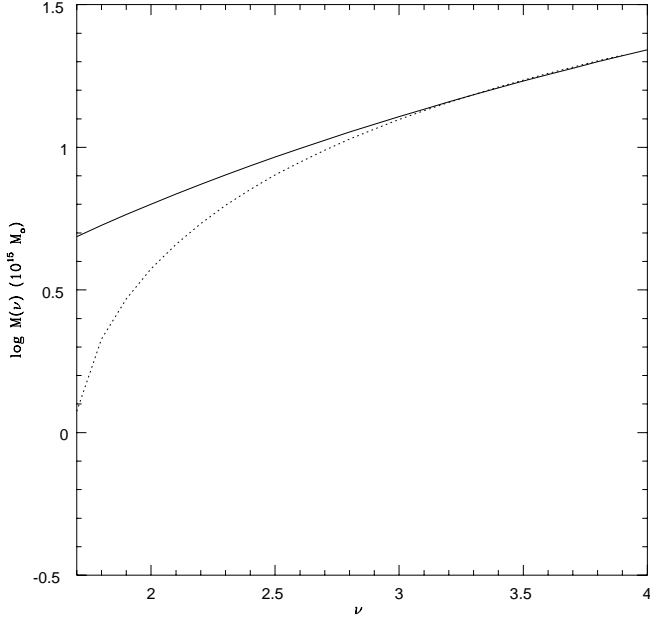


FIG. 4: The mass accreted by a collapsed perturbation, in units of  $10^{15} M_{\odot}$ , taking into account non-radial motions, dynamical friction and a non-zero cosmological constant (dotted line) compared to SM mass (solid line).

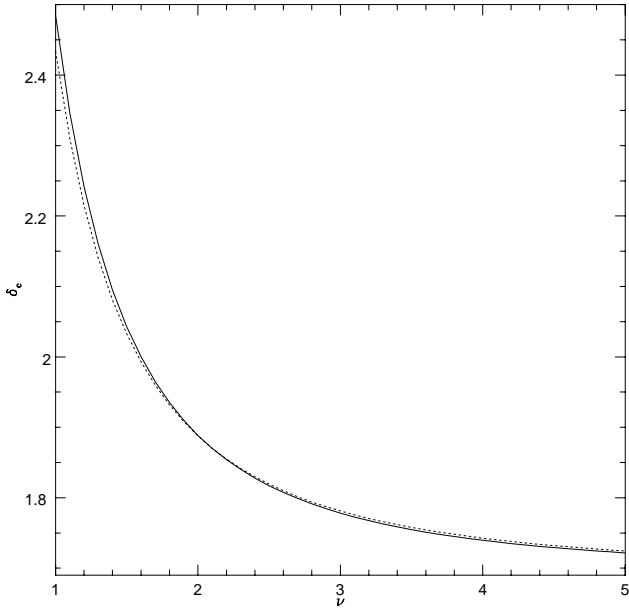


FIG. 5: The critical threshold,  $\delta_c(\nu)$  versus  $\nu$ . The dashed line is obtained with the model of the present paper while the solid line is that of ST.

by the relation:

$$dN = n(M)dM \quad (99)$$

that is the number of objects per unit volume, having a mass in the range  $M$  ed  $M + dM$ . The multiplicity function can also be used to define the luminosity function after having fixed the ratio  $\frac{M}{L}$ . Obtaining the mass function starting from that of luminosity is complicated since the ratio  $\frac{M}{L}$  is known with noteworthy uncertainty and it is different for different populations and different luminosity functions.

Finally trying to determine the luminosity function observationally is problematic (see for example [101]). For the above reasons, the theoretical determination of the mass function is very important. One of the most successful study in the subject is that of [51]. This theory is based upon these hypotheses:

- The linear density field is described by a stochastic Gaussian field. The statistics of the matter distribution is Gaussian.
- The evolution of density perturbations is that described by the linear theory. Structures form in those regions where the overdensity linearly evolved and filtered with a top-hat filter exceeds a threshold  $\delta_c$  ( $\delta_c = 1.68$ , obtained from the spherical collapse model ([53])).
- for  $\delta \geq \delta_c$  regions collapse to points. The probability that an object forms at a certain point is proportional to the probability that the point is in a region with  $\delta \geq \delta_c$  given by:

$$P(\delta, \delta_c) = \int_{\delta_c}^{\infty} d\delta \frac{1}{\sigma(2\pi)^{\frac{1}{2}}} \exp\left(-\frac{\delta^2}{2\sigma^2}\right) \quad (100)$$

The multiplicity function is given by:

$$\rho(M, z) = -\rho_0 \frac{\partial P}{\partial M} dM = n(M)M dM \quad (101)$$

If we add the conditions  $\Omega = 1$ ,  $|\delta_k|^2 \propto k^n$ , the Press-Schechter solution is autosimilar and has the form:

$$\rho(M, z) = \frac{\rho}{\sqrt{2\pi}} \left(\frac{n+3}{3}\right) \left(\frac{M}{M_*}(z)\right)^{\frac{n+3}{6}} \times \exp\left[-\frac{1}{2} \frac{M}{M_*}(z)^{\frac{n+3}{3}}\right] \frac{dM}{M} \quad (102)$$

where  $M_*(z) \propto (1+z)^{-\frac{6}{n+3}}$ . Several are the problems of the theory:

- **Statistical problems:** in the limit of vanishing smoothing radii, or of infinite variance, the fraction of collapsed mass, asymptotes to 1/2. This is a signature of linear theory: only initially overdense regions, which constitute half of the mass, are able to collapse. Nonetheless, underdense regions can be included in larger overdense ones, or, more generally, non-collapsed regions have a finite probability of being included in larger collapsed ones; this is commonly called *cloud-in-cloud problem*. PS argued that the missing mass would accrete on the formed structures, doubling their mass without changing the shape of the MF; however, they did not give a true demonstration of that. Then, they multiplied their MF by a “fudge factor” 2. Other authors used to multiply the MF by a factor  $(1+f)$ , with  $f$  denoting the fraction of mass accreted by the already formed structures.

- **Dynamical problems:** the heuristic derivation of the PS MF bypasses all the complications related to the highly non-linear dynamics of gravitational collapse. Spherical collapse helps in determining the  $\delta_c$  parameter and in identifying collapsed structures with virialized halos. However, the PS procedure completely ignores important dynamical elements, such as the effects of tidal forces, dynamical friction, and

that every structure virializes just after collapse is a crude simplification: when a region collapses, all its substructure is supposed by PS to be erased at once, while in realistic cases the erasure of substructures is connected to the two-body interaction of already collapsed clumps, an important piece of gravitational dynamics which is completely missed by the PS procedure.

- **Geometrical problems:** to estimate the mass function from the fraction of collapsed mass at a given scale it is necessary to relate the mass of the formed structure to the resolution

In practice, the true geometry of the collapsed regions in the Lagrangian space (i.e. as mapped in the initial configuration) can be quite complex, especially at intermediate and small masses; in this case a different and more sophisticated mass assignment ought to be developed, so that geometry is taken into account. For instance, if structures are supposed to form in the peaks of the initial field, a different and more geometrical way to count collapsed structures could be based on peak abundances.

Despite all of its problems, the PS procedure proved successful, as compared to N-body simulations, and a good starting point for all the subsequent works on the subject ([102]; [103], Bond et al. (1991), [104], [105], [106], [107], [69]. Most authors reported the PS formula to fit well their N-body results; nonetheless, all the authors agree in stating the validity of the PS formula to be only statistical, i.e. the existence of the single halos is not well predicted by the linear overdensity criterion of PS (see in particular Bond et al. 1991)). There are however some exceptions to this general agreement: [108] reported their MF, based on a CDM spectrum, to be very similar to a power-law with slope  $-2$ , different from the PS formula both at small and at large masses. Several authors, [105], [109] and [110] noted that, to make the PS formula agree with their simulations (based on CDM or CHDM spectra), it is necessary to lower the value of the  $\delta_c$  parameter as redshift increases. The same thing was found by [111], but was interpreted as an artifact of their clump-finding algorithm. Recent simulations seem to confirm this trend.

Lacey & Cole ([112]) extended the comparison to N-body simulations to the predictions for merging histories of dark-matter halos; they found again a good agreement between theory and simulations. This fact is noteworthy, as merging histories contain much more detailed information about hierarchical collapse. Several improvements of the theory exists: [106] (the so called Extended Press & Schechter (EPS) formalism; [113]).

### 1.11 CDM, HDM and others cosmogonies

The study of origin and formation of structure in the universe has been historically fundamentally framed into two theories: the CDM theory, in which WIMPS constitutes the main part of Dark Matter, and HDM in which neutrinos dominate. As we are going to see, structure formation in these scenarios is completely different since WIMPS and neutrinos are subject to different physical phenomena and then the transfer function is noteworthy different in the two cases. Both theories have the same starting points:

- 1) The universe is fundamentally constituted by Dark Matter (WIMPS in the CDM model and neutrinos in the HDM) and  $\rho = \rho_c$  ( $\Omega = 1$ ).

- 3) Fluctuations originating in the primordial universe are adiabatic, scale invariant,  $n = 1$ , and Gaussian ([28]).

If universe is dominated by neutrinos with mass  $m_\nu = 30\text{ev}$  the transfer function is determined by the free-streaming (or Landau damping) of neutrinos. This phenomenon consists in the smoothing of inhomogeneities in the primordial universe (due to perturbations in the acollisional components) because of the motion of neutrinos from overdense to underdense regions. Neutrinos diffusion and the smoothing of inhomogeneities is possible only before  $t = t_{eq}$ . After this epoch, there is no longer free-streaming but the density perturbation has definitely changed by its previous action. Free-streaming scale or mass can be estimated calculating the distance covered from a particle decoupled from plasma. Results that one obtains for the free-streaming scale and mass is ([13]):

$$\lambda_{FS} \approx 40\text{Mpc}(m_\nu/30\text{ev})^{-1} \quad M_{FS} \approx 10^{15}(m_\nu/30\text{ev})^{-2}M_0 \quad (103)$$

Because of free-streaming of neutrinos the HDM spectrum is characterized by a cut-off at short wave-length. The result is that the first objects that form are superclusters and structure formation proceeds because of fragmentation. [47] showed that the first structure to form are flat and were called "pancakes". After formation, these objects enter in the non-linear phase along one of the axes and baryons inside start to collide and dissipate their gravitational energy. Galaxies form for fragmentation processes. Structure formation follows a 'top-down' scheme, that means that larger objects (e.g., clusters) form before, while smaller objects (e.g., galaxies) later. N-body simulations of HDM universes ([114]; [115] showed that on scales larger than 10 Mpc structures is qualitatively similar to voids and to the filamentary structure that is visible in the CFA, but the clustering measured in N-body simulations is larger than that observed in the CFA. When one tries to reproduce the observed correlation function, one arrives to the conclusion that pancaking should have happened at redshift  $z \leq 1$ , in disagreement with observed galaxies having  $z \geq 1$  and QSO with  $z \geq 3$ . A further problem of the model is that of the peculiar velocity that are smaller than values obtained from observations ([13]).

The HDM model after a series of studies in the '80s has been abandoned for the problems it has and replaced by another model, the CDM, which is in better agreement with observations. The CDM model has a spectrum without a cut-off at short wave-length (at least till scales much smaller than galactic scales) because the damping scale is unimportant for WIMPS with mass  $> 1\text{Gev}$ . Structure formation is typically hierarchical: from smaller scale structure to larger ones. This scheme is a 'bottom-up' scheme. When the CDM model was introduced it obtained noteworthy successes in the description of the characteristic of the universe (clustering statistics of galaxies, peculiar velocities, CMBR fluctuations) from the galactic scale on ([116]; [117]; [52]; [118]; [119]; [28]). The model has shown some weak points, when compared with more and more precise data.

The reason of the success of the CDM model is fundamentally due to the fact that WIMPS interact with matter by means of gravity only, and does not feel the effect of pressure forces due to interaction with radiation (to which matter components are subject). Structure formation starts before in the CDM component, at  $t < t_{eq}$ , which give rise to the potential wells in which baryonic matter can then fall. It is important to notice that, in order to reproduce observations, additional mechanisms are needed, such as dark energy.



*mass.*<sup>6</sup> Typical problems of the CDM model in absence of biasing are the too high values for the r.m.s. of peculiar velocity of couple of galaxies (values of 1000 km/s vs.  $300 \pm 50$  km/s observed). Another problem is the correlation length,  $r_0$ , in N-body simulations, for the correlation function  $\xi$  which is equal to  $1.3h^{-1}Mpc$ , smaller than the observed value  $5.5h^{-1}Mpc$ . On the other side, if, in order to eliminate the quoted problems one introduce the biasing hypothesis, there is the supplementary problem of finding a physical mechanism that explains the origin of bias. Several conjectures has been proposed ([120]; [121]; [122]) but there is no full agreement on them.

Summarizing, one can tell that although at the beginning the standard form of CDM was very successful in describing the structures observed in the Universe (galaxy clustering statistics, structure formation epochs, peculiar velocity flows) ([116]; [117]; [52]; [118]; [119]; [28]) recent measurements have shown several deficiencies in the model, at least, when any bias of the distribution of galaxies relative to the mass is constant with scale (see [123]; [124]; [125], [126]). Some of the most difficult problems that must be reconciled with the theory are:

- the magnitude of the dipole of the angular distribution of optically selected galaxies ([127]);
- the possible observations of clusters of galaxies with high velocity dispersion at  $z \geq 0.5$  ([128]);
- the strong clustering of rich clusters of galaxies,  $\xi_{cc}(r) \simeq (r/25h^{-1}Mpc)^{-2}$ , far in excess of CDM predictions ([86]);
- the X-ray temperature distribution function of clusters, over-producing the observed clusters abundances ([98]);
- the conflict between the normalization of the spectrum of the perturbation which is required by different types of observations;
- the incorrect scale dependence of the galaxy correlation function,  $\xi(r)$ , on scales 10 to  $100 h^{-1}Mpc$ , having  $\xi(r)$  too little power on the large scales compared to the power on smaller scales ([129]; [130]; [131]; [132]).
- Normalization obtained from COBE data ([133]) on scales of the order of  $10^3 Mpc$  requires  $\sigma_8 = 0.95 \pm 0.2$ , where  $\sigma_8$  is the rms value of  $\frac{\delta M}{M}$  in a sphere of  $8h^{-1}Mpc$ . Normalization on scales 10 to  $50 Mpc$  obtained from QDOT and POTENT ([134]) requires that  $\sigma_8$  is in the range  $0.7 \div 1.1$ , which is compatible with COBE normalization while the observations of the pairwise velocity dispersion of galaxies on scales  $r \leq 3Mpc$  seem to require  $\sigma_8 < 0.5$ .
- Another problem of CDM model is the incorrect scale dependence of the galaxy correlation function,  $\xi(r)$ , on scales 10 to  $100 Mpc$ , having  $\xi(r)$  too little power on the large scales compared to the power on smaller scales. The APM survey ([129]), giving the galaxy angular correlation function, the 1.2 Jy IRAS power spectrum, the QDOT survey ([130]), X-ray observations ([135]) and radio observations

([131]; [132]) agree with the quoted conclusion. As shown in recent studies of galaxy clustering on large scales ([129]; [130]) the measured rms fluctuations within spheres of radius  $20h^{-1}Mpc$  have value 2-3 times larger than that predicted by the CDM model.

- Density profiles of CDM halos: the cusp obtained from numerical simulations seems too steep. -
- simulations might yield too many satellites for galaxies like our own. Though this second problem may have been the result of bad comparison of simulations with observations. This yielded a surge of interest in the last 2-3 years for Warm Dark matter and slightly collisional matter.

These discrepancies between the theoretical predictions of the CDM model and the observations led many authors to conclude that the shape of the CDM spectrum is incorrect and to search alternative models ([136]; [137]; [138]; [139]; [3]; [140]; [141]; [124]).

Alternative models with more large-scale power than CDM have been introduced in order to solve the latter problem. Several authors have lowered the matter density under the critical value ( $\Omega_m < 1$ ) ( $\Omega_m \simeq 0.3$ ) (this model is called open cold dark matter model (OCDM)) and others ([136]; Efstathiou et al. 1990a; [3]) have also added a cosmological constant in order to retain a flat Universe ( $\Omega_m + \Omega_\Lambda = 1$ ). This model is known as  $\Lambda$ CDM model. The spectrum of the matter density is specified by the transfer function, but its shape is affected because of the fact that the epoch of matter-radiation equality is earlier,  $1 + z_{eq}$  being increased by a factor  $1/\Omega_m$ . The epoch of matter-radiation equality is earlier, because  $1 + z_{eq}$  is increased by a factor  $1/\Omega_m$ . Around the epoch  $z_\Lambda$  the growth of the density contrast slows down and ceases after  $z_\Lambda$ . As a consequence the normalization of the transfer function begins to fall, even if its shape is retained (and pushes its imprint to larger scales). Mixed Dark Matter models (MDM) ([137]; [138]; [139]; [140]) increase the large-scale power because neutrinos free-streaming damps the power on small scales. Alternatively, changing the primeval spectrum several problems of CDM are solved ([141]). For example, in the  $\tau$ CDM model the needed changes in the power spectrum may be obtained in  $\Omega = 1$  CDM models if matter-radiation equivalence is delayed, such as by the addition of an additional relativistic particle species. Finally it is possible to assume that the threshold for galaxy formation is not spatially invariant but weakly modulated (2% – 3% on scales  $r > 10h^{-1}Mpc$ ) by large scale density fluctuations, with the result that the clustering on large-scale is significantly increased ([124]).

### 1.12 Constraints from recent astrophysical observations

In the past decade we have witnessed spectacular progress in precision measurements in astrophysics as a result of significant improvements in terrestrial and extraterrestrial instrumentation. The (second phase of the) Hubble telescope opened up novel paths in our quest for understanding the Universe, by allowing observations on distant corners of the observable Universe that were not accessible before.

From the point of view of interest to particle physics, the most spectacular claims from astrophysics came 8 years ago from the study of distant supernovae (redshifts  $z \sim 1$ ) by two independent groups [142]. These observations pointed towards a current era acceleration of our Universe, something that could be achieved with dark energy.

Universe, or in general by a non-zero *dark energy* component, which could even be relaxing to zero (the data are consistent with this possibility). This claim, if true, could revolutionize our understanding of the basic physics governing fundamental interactions in Nature. Indeed, only a few years ago, particle theorists were trying to identify (alas in vain!) an exact symmetry of nature that could set the cosmological constant (or more generally the vacuum energy) to zero. Now, astrophysical observations point to the contrary. The skeptics may question the accuracy of the supernovae observations, however, there is additional evidence from quite different in origin astrophysical observations, those associated with the measurement of the cosmic microwave background radiation (CMB), which point towards the fact that 73 % of the Universe vacuum energy consists of a dark (unknown) energy substance, in agreement with the (preliminary) supernovae observations. Moreover, recently [143] two more distant supernovae have been discovered ( $z > 1$ ), exhibiting similar features as the previous measurements, thereby supporting the geometric interpretation on the acceleration of the Universe today, and arguing against the nuclear physics or intergalactic dust effects.

Above all, however, there are the very recent data from a new probe of Cosmic Microwave Background Radiation Anisotropy (Wilkinson Microwave Anisotropy Probe (WMAP)) [144]. In its first year of running WMAP measured CMB anisotropies to an unprecedented accuracy of billionth of a Kelvin degree, thereby correcting previous measurements by the Cosmic Background Explorer (COBE) satellite [145] by several orders of magnitude. This new satellite experiment, therefore, opened up a new era for astroparticle physics, given that such accuracies allow for a determination (using best fit models of the Universe) of cosmological parameters [146], and in particular cosmological densities, which, as we shall discuss in this review, is quite relevant for constraining models of particle physics to a significant degree.

The WMAP satellite experiment determined the most important cosmological parameters that could be of relevance to particle physicists, namely [146]: the Hubble constant, and thus the age of the Universe, the thickness of the last scattering surface, the dark energy and dark matter content of the Universe (to an unprecedented accuracy), confirming the earlier claims from supernovae Ia data [142], and provided evidence for early reionization ( $z \sim 20$ ), which, at least from the point of view of large scale structure formation, excludes Warm Dark Matter particle theory models.

An important comment concerns the dark energy component (73 %) of the Universe. The WMAP measured equation of state for the Universe  $p = w\rho$ , with  $p$  the pressure and  $\rho$  the energy density, implies  $-1 \leq w < -0.78$  (assuming the lower bound for theoretical reasons, otherwise the upper limit may be larger [146]). For comparison we note that  $w = -1$  characterizes a perfect fluid Universe with non-zero, positive, cosmological constant. As we shall remark, supergravity quintessence models do have this feature of  $w \rightarrow -1$ , and it may well be that by exploiting further the data on this dark energy component of the Universe one may arrive at the physically correct supergravity model which could constrain the supersymmetric particle physics models.

The results of the WMAP analysis (alone), including directly measurable and derived quantities, are summarized in the tables appearing in figures 7,8.

One therefore obtains the chart for the energy and matter content of our Universe depicted in figure 6. This chart is in perfect agreement with the earlier claims of the acceleration of the Universe.

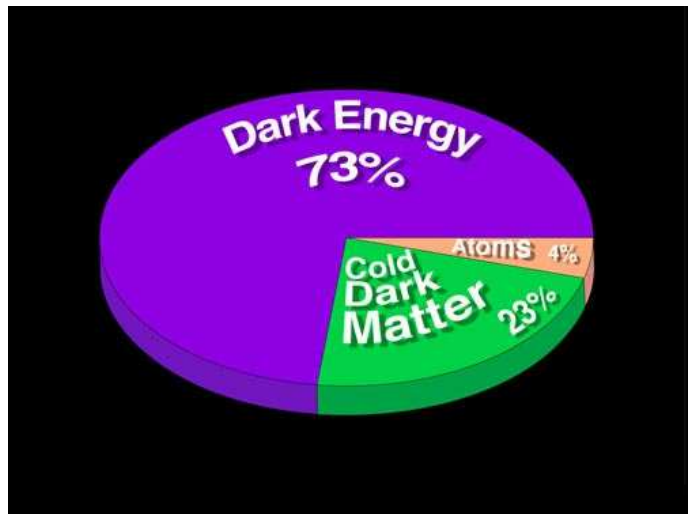


FIG. 6: The energy content of our Universe as obtained by fitting data of WMAP satellite. The chart is in perfect agreement with earlier claims made by direct measurements of a current era acceleration of the Universe from distant supernovae type Ia (courtesy of <http://map.gsfc.nasa.gov/>).

TABLE 1  
POWER LAW  $\Lambda$ CDM MODEL PARAMETERS- WMAP DATA ONLY

Parameter		Mean (68% confidence range)	Maximum Likelihood
Baryon Density	$\Omega_b h^2$	$0.024 \pm 0.001$	0.023
Matter Density	$\Omega_m h^2$	$0.14 \pm 0.02$	0.15
Hubble Constant	$h$	$0.72 \pm 0.05$	0.68
Amplitude	$A$	$0.9 \pm 0.1$	0.80
Optical Depth	$\tau$	$0.166^{+0.076}_{-0.071}$	0.11
Spectral Index	$n_s$	$0.99 \pm 0.04$	0.97
	$\chi^2_{eff}/\nu$		1431/1342

<sup>a</sup>Fit to WMAP data only

FIG. 7: Cosmological parameters measured by WMAP (only):directly measurable quantities [146].

novae Ia Data [142].

It should be stressed that the interpretation of the supernovae data is based on a *best fit* Friedmann-Robertson-Walker (FRW) Universe [142]:

$$0.8\Omega_M - 0.6\Omega_\Lambda \simeq -0.2 \pm 0.1, \quad \text{for } \Omega_M \leq 1.5 \quad (104)$$

with  $\Omega_{M,\Lambda}$  corresponding to the matter and cosmological matter densities. Assuming a flat model ( $k=0$ ),  $\Omega_{\text{total}} = 1$ , as supported by the CMB data, the SNIa data alone imply:

$$\Omega_M^{\text{Flat}} = 0.28^{+0.09}_{-0.08} (1\sigma \text{ stat.})^{+0.05}_{-0.04} (\text{identified syst.}) \quad (105)$$

The deceleration parameter defined as  $q \equiv -\frac{\ddot{a}a}{\dot{a}^2}$ , where  $a$  is the cosmic scale factor, receives the following form if we omit the contribution of photons which is very small,

$$q = \frac{1}{2}\Omega_M - \Omega_\Lambda \simeq -0.57 < 0, \quad (\Omega_\Lambda \simeq 0.7). \quad (106)$$

Hence (104) and (105) provide evidence for a *current era acceleration of the Universe*. At this stage it should be stressed that the recent observation of two more supernovae [143] further supports the acceleration of the Universe.

TABLE 1  
DERIVED COSMOLOGICAL PARAMETERS

Parameter	Mean (68% confidence range)
Amplitude of Galaxy Fluctuations	$\sigma_8 = 0.9 \pm 0.1$
Characteristic Amplitude of Velocity Fluctuations	$\sigma_8 \Omega_m^{0.6} = 0.44 \pm 0.10$
Baryon Density/Critical Density	$\Omega_b = 0.047 \pm 0.006$
Matter Density/Critical Density	$\Omega_m = 0.29 \pm 0.07$
Age of the Universe	$t_0 = 13.4 \pm 0.3$ Gyr
Redshift of Reionization (ionization fraction, $x_e = 1$ )	$z_r = 17 \pm 5$
Redshift at Decoupling	$z_{dec} = 1088_{-2}^{+1}$
Age of the Universe at Decoupling	$t_{dec} = 372 \pm 14$ kyr
Thickness of Surface of Last Scatter	$\Delta z_{dec} = 194 \pm 2$
Thickness of Surface of Last Scatter	$\Delta t_{dec} = 115 \pm 5$ kyr
Redshift at Matter/Radiation Equality	$z_{eq} = 3454_{-302}^{+385}$
Sound Horizon at Decoupling	$r_s = 144 \pm 4$ Mpc
Angular Diameter Distance to the Decoupling Surface	$d_A = 13.7 \pm 0.5$ Gpc
Acoustic Angular Scale( $l_A = \pi d_A / r_s$ )	$\ell_A = 299 \pm 2$
Current Density of Baryons	$n_b = (2.7 \pm 0.1) \times 10^{-7} \text{ cm}^{-3}$
Baryon/Photon Ratio	$\eta = (6.5_{-0.3}^{+0.4}) \times 10^{-10}$

FIG. 8: Cosmological parameters measured by WMAP (only):derived quantities [146].

and argues rather against the rôle of nuclear (evolution) or intergalactic dust effects.

The recent data of WMAP satellite lead to a new determination of  $\Omega_{\text{total}} = 1.02 \pm 0.02$ , where  $\Omega_{\text{total}} = \rho_{\text{total}}/\rho_c$ , due to high precision measurements of secondary (two more) acoustic peaks as compared with previous CMB measurements. Essentially the value of  $\Omega$  is determined by the position of the first acoustic peak in a Gaussian model, whose reliability increases significantly by the discovery of secondary peaks and their excellent fit with the Gaussian model [146].

## 2. CONCLUSIONS

This paper provides a review of the variants of dark matter which are thought to be fundamental components of the universe and their role in origin and evolution of structures. It moreover gives some new original results concerning improvements to the spherical collapse model. In particular, how the spherical collapse model is modified when we take into account dynamical friction and tidal torques. Studies of several decades have shown that, if we have a right knowledge of the law of gravity, dark matter is a fundamental component of our universe. While models based upon Hot Dark Matter (e.g., neutrinos) gives a reasonable description of structures on large scales models based upon Cold

Dark Matter (e.g., axions) are more successful in describing small and intermediate scales. A fundamental ingredient in the recipe of structure formation is inflation which provides a spectrum of adiabatic Gaussian perturbations which can be well described by a power-law spectrum, tilted from the Harrison–Zel’dovich spectrum, normally tilted so as to provide extra large scale power. The magnitude of the tilt may be modest or pronounced. The details of structure formation are very sensitive to the matter content of the universe. It appears that if cold dark matter is the main constituent of the universe, present observations require that the initial perturbations be adiabatic — isocurvature perturbations generate excessively large cmb anisotropies for the same final density perturbation. Adiabatic perturbations are exactly what inflation provides. In CDM models, the only remaining alternative would appear to be texture seeded models, which have been placed in jeopardy by a combination of microwave anisotropy and velocity data, though the death blow apparently remains to be struck. The survey was completed by examining variants on the CDM model which may be better suited to explaining the observational data. The standard technique is to utilize additional matter (be it a component of hot dark matter or of a cosmological constant) to remove short-scale power from the CDM spectrum. Hot dark matter does this by free-streaming, a cosmological constant by delaying matter-radiation equality. Because this power can be removed over a much shorter range of scales than with tilt, it enables an explanation of the observed deficit of short-scale power relative to intermediate scale power in the spectrum.

MDM (Mixed dark Model) adds yet another new parameter, roughly speaking an ability to remove short-scale power from the spectrum while leaving large scales untouched, and may be necessary should all present observations stand up. It appears likely that MDM will however need an initial spectrum close to  $n = 1$  with no gravitational waves if it is to succeed. Some studies ([136]; Efstathiou et al. 1990a; [3]) has shown that lowering the matter density under the critical value ( $\Omega_m < 1$ ) and adding a cosmological constant in order to retain a flat Universe ( $\Omega_m + \Omega_\Lambda = 1$ ), gives good results in the case of  $\Omega_m = 0.3$ . Moreover new observational evidences (see [147]) indicates that we are living in a  $\Lambda \neq 0$  universe.

## ACKNOWLEDGMENTS

The author thanks the referee M. V. Sazhin for his helpful comments.

- [1] Sciamia, D.W., 1984, Proc.R Soc.Lond. A 394, 1.
- [2] Bowyer S., Korpela E.J., Edelman J., Lampton M., Morales C., Perez-Mercader J., Gomez J.F., Trapero J., 1999, ApJ 526, 10
- [3] Turner, M.S., 1991, Physica scripta. vol T36, 167
- [4] Oort, J., H., 1932, Bull.Astr.Insts.Neth., 6, 249
- [5] Zwicky, F., 1933, Helvetica Physica Acta, 6, 110
- [6] Smith, S., 1936, Ap.J 83, 23
- [7] Friedmann, A., 1924, Z.Phys, 10, 377 e Z.Phys 1924, 21, 326.
- [8] Einstein, A., 1915, Preuss.Akad.Wiss.Berlin, Sitzber., 844.
- [9] Weyl, H., 1923, Z.Phys., 24, 230.
- [10] van Albada, T.S., Sancisi, R., 1986, Phil.Trans.R.Lond. A 320, 447.
- [11] Peebles, P.J.E., 1971, Physical cosmology, Princeton University Press, Princeton.
- [12] Guth, A.H., 1981, Phys. Rev D23, 347
- [13] Kolb, E.W., Turner, M.S., 1990, The Early Universe (Addison-Wesley)
- [14] Loh, E., Spillar, E.J., 1986, Ap.J 307 L1
- [15] Valageas P., 2000, A&A 354, 767
- [16] Dekel A., Burstein D., White S.D.M., 1996, proceedings of the Princeton 250th Anniversary conference, June 1996, ed. N. Turok (World Scientific), page 175,
- [17] Bahcall N.A., Fan X., Cen R., 1997, ApJ 485, 53
- [18] Ferreira P.G., Juszkiewicz R., Feldman H.A., Davis M., Jaffe A.H., 1999, ApJ 515, 1
- [19] Melchiorri et al., 2000, ApJ 536, 63
- [20] Branchini E., Zehavi I., Plionis M., Dekel A., 2000, MN-RAS 313, 491
- [21] Guth, A.H., 1981, Phys. Rev D23, 347
- [22] Linde, A., 1983, Phys.Lett B 129, 177.

- [24] Guth, A.H., Pi, S.Y., 1982, Phys.Rev.Lett. 49, 1110.
- [25] Hawking, S.W., Phys.Lett B 115, 295.
- [26] Starobinsky, A.A., 1982, Phys.Lett. B 117, 175.
- [27] Melchiorri A., Sazhin M. V., Shulga V. V., Vittorio N., 1999, ApJ 518, 562
- [28] Efstathiou, G., 1990, in " The physics of the early Universe", eds Heavens, A., Peacock, J., Davies, A. (SUSSP)
- [29] Finzi, A., 1963, MNRAS, 127, 21
- [30] Milgrom, M., 1983, Ap.J, 270, 365
- [31] Sanders, R.H., 1984, Astron.Astrophys, 136, L21
- [32] Lee, B.W., Weimberg, S., 1977, Phys.Rev.Lett 39, 165
- [33] Lyubimov ,V.A, Novikov, E.G., Nozik, V.Z., Tretyakov, E.G., Kosik, V.S., 1980, Phys.Lett. B, 94, 266
- [34] Jelley, N.A., 1986, Phil. Trans. R. soc. London. A, 320, 487
- [35] Zuber K., 1998, Phys.Rept. 305, 295-364
- [36] Peccei-Quinn, H.R., 1977, Phys.Rev.Lett, 38, 1440
- [37] Jeans, J.H., 1902, Phil.Trans.R.Soc. 199 A, 49.
- [38] Peebles, P.J.E., 1980, The large scale structure of the universe, Princeton University Press, Princeton.
- [39] Fry, J.N, 1982, Ap.J 262, 424
- [40] Davis, M., Peebles, P.J.E., 1978, Ap.J supplement series, 34, 425
- [41] Silk, J., 1968, Ap.J 151, 459.
- [42] Bond J.R., Efstathiou G., 1984, ApJ (Letters) 285, L45
- [43] Juskievicz, R., Sonoda, D.H., Barrow, J.D., 1984, MNRAS 209, 139
- [44] Kibble, T.W.B., Turok, N.G., 1986, Phil.Trans.R.Soc.Lond. A 320, 565
- [45] Suto, Y., Sato, K., Kodama, H., 1985: Prog.Theor.Phys. 73, 1151
- [46] Gouda, N., Sasaki, M., 1986: RiFP-preprint (Kyoto)
- [47] Zel'dovich, Ya. B., 1970, Astron. Astrophys 5, 84
- [48] West, M.J., Dekel, A., Oemler, A. Jr., 1987, Ap.J 316, 1.
- [49] Efstathiou, G., Silk, J., 1983, Fundamentals of cosmic Physics, 9, 1
- [50] Gurbatov, S.N., Saichev, A.I., Shandarin, S.F., 1985, Sov.Phys.Dokl. 30, 921.
- [51] Press, W.H, Schechter, P.L, 1974, Ap.J 187, 425
- [52] Bardeen, J.M, Bond, J.R., Kaiser, N., Szalay, A.S., 1986, Ap.J 304, 15
- [53] Gunn, J.E., Gott, J.R., 1972, Ap.J 176, 1
- [54] Bernardeau, S., 1994, ApJ 427, 51
- [55] Valageas P., 2002a, A&A, 382, 412
- [56] Valageas P., 2002a, A&A, 382, 450
- [57] Hoffman, Y., Shaham, J., 1985, Ap J, 297, 16
- [58] Ryden, B. S., 1988a, ApJ 329, 589
- [59] Ryden, B.S., 1988b, ApJ 333, 78
- [60] Kashlinsky, A., 1986, Ap. J. 306, 374
- [61] Kashlinsky, A., 1987, Ap. J., 312, 497
- [62] Peebles, P. J. E., 1990, ApJ, 365, 27
- [63] White, S. D. M., 1976, MNRAS 174, 19
- [64] Antonuccio V., Colafrancesco S., 1994, ApJ 427, 72 (AC)
- [65] Davis, M., Peebles, P.J.E., 1977, ApJ Suppl. 34, 425
- [66] Barrow, J. D., Silk, J., 1981, ApJ, 250, 432
- [67] Szalay, A. S., Silk, J., 1983, ApJ (Letters), 264, L31
- [68] Villumsen, J. V., Davis, M., 1986, ApJ 308, 499
- [69] Bond J.R., Myers S.T., 1996b, ApJS, 103, 41
- [70] Lokas E.L., Juskievicz R., Bouchet F.R., Hivon E., 1996, ApJ, 467, 1
- [71] Hoffman, Y.: (1986), ApJ, 301, 65
- [72] Evrard, A.E., Crone, M.M., 1992, ApJ, 394, L1
- [73] Bertschinger, E. and Jain, B., 1994, ApJ 431, 486
- [74] Monaco P., 1995, ApJ, 447, 23
- [75] Audit, E., Teyssier, R. and Alimi, J. M., 1997, A&A, 325, 439
- [76] Del Popolo, A., E. N. Ercan, Z. Q. Xia, 2001, AJ 122, 487
- [77] Del Popolo A., 2002, A&A 387, 759
- [78] Icke V., 1973, A&A 27, 1
- [79] White, S.D.M. and Silk, J., 1979, ApJ 231, 1
- [80] Watanabe, T., 1993, Pasj 45, 393
- [81] Kashlinsky, A., 1984, MNRAS 208, 623
- [82] Chandrasekhar, S., von Neumann, J., 1942, ApJ, 95, 489
- [83] Kandrup, H.E., 1980, Phys. Rep. 63, n 1, 1
- 392, 403
- [85] Peacock, J.A., Heavens, A.F., 1990, MNRAS 243, 133
- [86] Bahcall N.A., Soneira R.M., 1983, ApJ 270, 20
- [87] Postman, M., Geller, M. J., Huchra, J. P., 1986, ApJ, 91, 1267
- [88] Davis, M., Peebles, P. J. E., 1983, Ap J, 267, 465
- [89] Gonzalez A. H., Zaritsky D., Wechsler R., 2002ApJ...571..129
- [90] Hoyle, F.: (1949), in IAU and International Union of Theoretical and Applied Mechanics Symposium, p. 195
- [91] Peebles, P. J. E., (1969), ApJ 155, 393
- [92] White, S. D. M., 1984, ApJ 286, 38
- [93] Eisenstein D.J., Loeb A., 1995, ApJ 439, 250
- [94] Catelan P., Theuns T., 1996a, MNRAS 282, 436
- [95] Catelan P., Theuns T., 1996b, MNRAS 282, 455
- [96] Barnes, J., Efstathiou, G., 1987, ApJ, 319, 575
- [97] Peebles, P. J. E., 1993, Principles of Physical Cosmology, Princeton University Press
- [98] Bartlett J.G., Silk J., 1993, ApJ 407, L45
- [99] Colafrancesco, S., Antonuccio, V., Del Popolo, A., 1995, ApJ 455, 32
- [100] Sheth R. K., Tormen G., 1999, MNRAS 308, 119 (ST)
- [101] Efstathiou, G., Ellis, R.S., Peterson, B.A., 1988, MNRAS 232, 431
- [102] Efstathiou G., Frenk C.S., White S.D.M., Davis M., 1988, MNRAS, 235,
- [103] Efstathiou G., Rees M.J., 1988, MNRAS, 230, 5P
- [104] White S.D.M., Efstathiou G., Frenk C.S., 1993, MNRAS, 262, 1023
- [105] Jain B., Bertschinger E., 1994, ApJ, 431, 495
- [106] Lacey C., Cole S., 1993, MNRAS, 262, 627
- [107] Efstathiou G., 1995, MNRAS, 272, L25
- [108] Brainerd T.G., Villumsen J.V., 1992, ApJ, 394, 409
- [109] Gelb J.M., Bertschinger E., 1994, ApJ, 436, 467
- [110] Ma C., Bertschinger E., 1994, ApJ, 434, L5
- [111] Klypin A., Borgani S., Holtzman J., Primack J., 1995, ApJ, 444, 1
- [112] Lacey C., Cole S., 1994, MNRAS, 271, 676
- [113] Sheth R. K., Tormen G., 2002, MNRAS 329, 61 (ST1)
- [114] Frenk, C.S., White, S.D.M., Davis, M., 1983, Ap.J 271, 417
- [115] Centrella, J., Mellot, A.L., 1983, Nature, Lond., 305, 196
- [116] Peebles, P.J.E., 1982b, Ap.J, Lett. 263, L1
- [117] Blumenthal, G.R., Faber, S.M., Primack, J.R., Rees, M.J., 1984, Nature 311, 517
- [118] White, D.M., Frenk, C.S., Davis, M., Efstathiou, G.,
- [119] Frenk, C.S., White, S.D.M., Efstathiou, G., 1988, Ap.J. 327, 507
- [120] Rees, M.J., 1985, MNRAS, 213, 75p
- [121] Silk, J., 1985, Ap.J 297, 1
- [122] Dekel, A., Rees, M., 1987, Nature 326, 455
- [123] Babul A., White S.D.M., 1991, MNRAS 253, 31P
- [124] Bower R.G., Coles P., Frenk C.S., White S.D.M., 1993, ApJ 405, 403
- [125] Del Popolo A., Gambera M., 1998, A&A 337, 96
- [126] Del Popolo A., Gambera M., 1998b, Proceedings of the VIII Conference on Theoretical Physics: General Relativity and Gravitation - Bistritza - June 15-18, 1998 - Romania
- [127] Kaiser N., Lahav O., 1989, MNRAS 237, 129
- [128] Evrard A.E., 1989, ApJ 341, L71
- [129] Maddox S.J., Efstathiou G., Sutherland W.J., Loveday J., 1990a, MNRAS 242, 43p
- [130] Saunders, W., Frenk C., Rowan-Robinson M. et al., 1991, Nature 349, 32
- [131] Peacock J.A., 1991, MNRAS 253, 1p
- [132] Peacock J.A., Nicholson D., 1991, MNRAS 253, 307
- [133] Smoot G.F., Bennett C.L., Kogut A. et al., 1992, ApJ 396, L1
- [134] Dekel A., Bertschinger E., Yahil A. et al., 1992, IRAS galaxies versus POTENT mass: density fields, biasing and  $\Omega$ , Princeton preprint IASSNS-AST 92/55
- [135] Lahav O., Edge A., Fabian A.C., Putney A., 1989, MNRAS 238, 881
- [136] Peebles P.J.E., 1984, ApJ 284, 439

- [138] Valdarnini R., Bonometto S.A., 1985, A&A 146, 235
- [139] Holtzman J., 1989, ApJS 71, 1
- [140] Schaefer R.K., 1991, Int. J. Mod. Phys. A6, 2075
- [141] Cen R.Y., Gnedin N.Y., Kofman L.A., Ostriker J.P., 1992 preprint
- [142] B. P. Schmidt *et al.*, Astrophys. J. **507** (1998) 46 [arXiv:astro-ph/9805200]; S. Perlmutter *et al.* [Supernova Cosmology Project Collaboration], Astrophys. J. **517** (1999) 565 [arXiv:astro-ph/9812133]; J. P. Blakeslee *et al.*, Astrophys. J. **589** (2003) 693 [arXiv:astro-ph/0302402]; A. G. Riess *et al.*, Astrophys. J. **560** (2001) 49 [arXiv:astro-ph/0104455].
- [143] S. Perlmutter and B. P. Schmidt, arXiv:astro-ph/0303428; J. L. Tonry *et al.*, arXiv:astro-ph/0305008.
- [144] C. L. Bennett *et al.*, arXiv:astro-ph/0302207.
- [145] G. F. Smoot *et al.*, Astrophys. J. **396**, L1 (1992); C. L. Bennett *et al.*, Astrophys. J. **436**, 423 (1994) [arXiv:astro-ph/9401012];
- [146] D. N. Spergel *et al.*, arXiv:astro-ph/0302209.
- [147] Corasaniti P.S., , Copeland E.J., 2002, PhRvD 65, d300

<sup>a</sup> See Dekel et al. 1996 for a discussion of the table.  $\sigma_8$  is the *rms* mass density fluctuation in a top-hat sphere of radius  $8h^{-1}Mpc$ .  
<sup>b</sup>  $\beta \equiv \Omega^{0.6}/b$ ,  $b_I$  for IRAS galaxies,  $b_o$  for optical galaxies.  
<sup>c</sup>  $b_o/b_I \simeq 1.3$ ,  $b_o \simeq 1/\sigma_8$ .

**Table 3: Estimates of  $\Omega_m$** 

Global Measures	Inflation, Occam	$\Omega_m + \Omega_\Lambda = 1$ ( $\Omega_m = 1, \Omega_\Lambda = 0$ )
	Luminosity distance SNIa	$-0.3 < \Omega_m - \Omega_\Lambda < 2.5$ (90%)
	Lens Counts	Flat $\Omega_m > 0.49$ (95%)
	CMB Peak	Flat $\Omega_m > 0.34$ (95%)
	$H_0 t_0$	$\Omega_m + \Omega_\Lambda < 1.5$ (95%) $\Omega_m + \Omega_\Lambda > 0.3$ (likely $\sim 0.7$ ) $\Omega_m - 0.7\Omega_\Lambda < 1.3$ (likely $\leq 0$ )
Virialized Objects	$(M/L)\mathcal{L}$	$\Omega_m \sim 0.25$ (0.1 – 1.0)
	Baryon fraction	$\Omega_m h_{65}^{1/2} \sim 0.3 - 0.5$ (low–high $\Omega_b$ )
	Cosmic Virial Th.	Point mass $\Omega_m \sim 0.2$ (halos $\rightarrow 1$ )
	Local Group	Point mass $\Omega_m \sim 0.15$ (halos $\rightarrow 0.7$ )
Large-Scale; Flows	Peculiar velocities	$\Omega_m > 0.3$ (95%) $\Omega_m^{0.6} \sigma_8^g = 0.8 \pm 0.2$ ( $\beta_I^g \simeq 1.05^c$ )
	Redshift Distortions	$\beta_I \sim 0.5 - 1.2$
	Velocity vs Density	$\beta_I \sim 0.5 - 1.2$ (scale dependent)
	Cluster Abundance	$\beta_o \sim 0.4 - 0.95$ $\Omega_m^{0.6} \sigma_8 \simeq 0.5 - 0.6$ ( $\beta_I \simeq 0.7 - 0.8^c$ )
Fluctuation Growth	Cluster Morphology	$\Omega_m > 0.2$ (?)
	Galaxy Formation	(?)
	$P_k(\rho)$ vs $C_l$	CDM $n = 1$ $b = 1$ : $\Omega_m h_{65} \sim 0.3$
	$P_k(v)$ vs $C_l$	CDM flat: $\Omega_m h_{65} n^2 \simeq 0.7 \pm 0.1$

